



## **Changes in seasonality of groundwater level fluctuations in a temperate-cold climate transition zone**

Downloaded from: <https://research.chalmers.se>, 2026-04-04 15:24 UTC

Citation for the original published paper (version of record):

Nygren, M., Giese, M., Klöve, B. et al (2020). Changes in seasonality of groundwater level fluctuations in a temperate-cold climate transition zone. *Journal of Hydrology*, 8. <http://dx.doi.org/10.1016/j.hydroa.2020.100062>

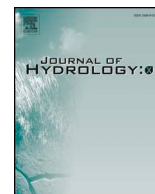
N.B. When citing this work, cite the original published paper.



ELSEVIER

Contents lists available at ScienceDirect

Journal of Hydrology X

journal homepage: [www.journals.elsevier.com/journal-of-hydrology-x](http://www.journals.elsevier.com/journal-of-hydrology-x)

## Research papers

## Changes in seasonality of groundwater level fluctuations in a temperate-cold climate transition zone

Michelle Nygren<sup>a,\*</sup>, Markus Giese<sup>a</sup>, Bjørn Kløve<sup>b</sup>, Ezra Haaf<sup>a</sup>, Pekka M. Rossi<sup>b</sup>, Roland Barthel<sup>a</sup><sup>a</sup> Department of Earth Sciences, University of Gothenburg, Guldhedsgatan 5A, 41320 Gothenburg, Sweden<sup>b</sup> Water, Energy and Environmental Engineering Research Unit, University of Oulu, Pentti Kaiterankatu 1, 90570 Oulu, Finland

## ARTICLE INFO

This manuscript was handled by Corrado Corradini, Editor-in-Chief, with the assistance of Patrick Lachassagne, Associate Editor

## Keywords:

Groundwater level fluctuations  
Climate change  
Dynamic groundwater storage  
Snowmelt recharge  
Fennoscandia

## ABSTRACT

In cold (i.e. boreal, subarctic, snowy) climate zones, dynamic groundwater storage is greatly affected by the timing and amount of snowmelt. With global warming, cold climates in the northern hemisphere will transition to temperate. As temperatures rise, the dominant type of precipitation will change from snow to rain in winter. Further, the growing season is prolonged. This has a direct impact on the aquifer recharge pattern. However, little is known about the effect of changing annual recharge regimes on groundwater storage.

The present work deduces the impact of shifting climate zones on groundwater storage by evaluating the effect of climate seasonality on intra-annual hydraulic head fluctuations. The work compares intra-annual hydraulic head fluctuations in a temperate-cold climate transition zone (Fennoscandia) from two different periods (1980–1989, 2001–2010). This is done by associating rising vs. declining hydraulic heads with hydro-meteorology.

Due to the northwards migration of the temperate climate zone, there is a shift in seasonality between the two periods. This has a negative impact on groundwater levels, which are significantly lower in 2001–2010, particularly near the climate transition zone. The results demonstrate that increasing temperatures in cold climate regions may change the seasonality of groundwater recharge, by altering the main recharge period from being snowmelt-dominated (spring) to rain-dominated (winter). Additionally, this is connected to the duration of the growing season, which impedes groundwater recharge. The coupled effect of this on groundwater in the study area has led to a significant decrease in groundwater storage.

## 1. Introduction

Climate change impact studies on groundwater resources generally use the output of global climate models (GCMs) as input to hydrological models (e.g.: Scibek and Allen, 2006; Jyrkama and Sykes, 2007; Scibek et al., 2007; Clilverd et al., 2011; Surfleet et al., 2012; Kurylyk and MacQuarrie, 2013; Surfleet and Tullios, 2013; Meixner et al., 2016). This approach is partly justified since the study of significant trends require long time series (Stoll et al., 2011). Most groundwater observations do not fit this requirement, which also does not allow for cross-validation against model results. As a consequence, results indicate wildly varying possibilities for future change ranging from decreasing (e.g. Sultana and Coulibaly, 2011; Luoma and Okkonen, 2014; Jang et al., 2015) over stable (e.g. Scibek and Allen, 2006; Scibek et al., 2007; Meixner et al., 2016) to increasing (e.g. Jyrkama and Sykes, 2007; Kovalevskii, 2007; Clilverd et al., 2011) groundwater storage or recharge. This variability is highly connected to uncertainty with regard

to initialisation and parameterisation of processes known to heavily affect future groundwater recharge estimates. These uncertainties are associated with [1] global precipitation patterns, climate change scenarios and discrepancies between GCMs (Surfleet et al., 2012; Surfleet and Tullios, 2013); [2] the dependency on the type of downscaling method used (Chen et al., 2006; Baba et al., 2011; Kurylyk and MacQuarrie, 2013); and [3] insufficient understanding of atmosphere-groundwater interactions (Green et al., 2011; Kløve et al., 2014). In addition, output in the form of annual or longer-term averages of groundwater recharge, common for climate change impact studies, portray neither extremes nor seasonal variations of recharge/storage.

Seasonal variability of groundwater recharge/storage may develop into groundwater-related hazards, such as floods, water scarcity and drought (Taylor et al., 2012). Any of these effects results in increased pressure on important groundwater-dependent ecosystems (Taylor et al., 2012; Jyväsjärvi et al., 2015), communities and industry. Their ability to adjust to future changes in water availability is reliant on the

\* Corresponding author.

E-mail address: [michelle.nygren@gu.se](mailto:michelle.nygren@gu.se) (M. Nygren).<https://doi.org/10.1016/j.hydroa.2020.100062>

Received 22 May 2020; Received in revised form 3 August 2020; Accepted 4 August 2020

Available online 08 August 2020

2589-9155/© 2020 The Authors. Published by Elsevier B.V. This is an open access article under the CC BY license (<http://creativecommons.org/licenses/by/4.0/>).

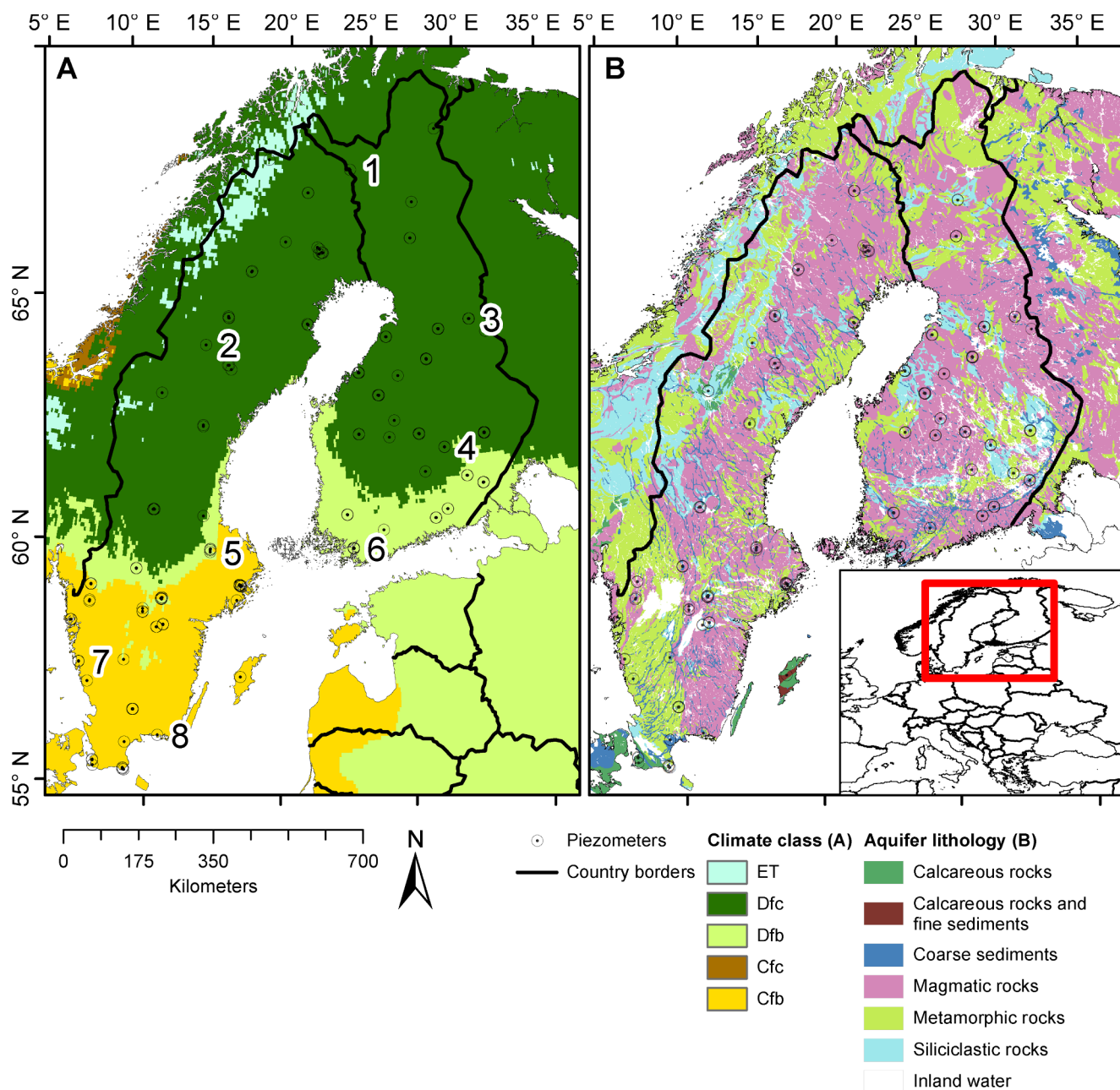


Fig. 1. A) Köppen-Geiger climate classes in the Swedish and Finnish parts of Fennoscandia based on Kottke et al (2006) and Rubel et al (2017). Circles represent piezometers. Cfb – temperate humid warm summers; Cfc – temperate humid cold summers; Dfb – cold humid warm summers; Dfc – cold humid cold summers; ET – Arctic tundra climate. Annotated piezometer groups (numbers) are used as examples to highlight results from the classification. B) Aquifer lithology based on the European geological map of Asch (2003).

rate of change and, more importantly, their ability to adapt (Kirkinen et al., 2005; Kjellström et al., 2014; Kløve et al., 2017). Consequently, changes in intra-annual groundwater fluctuations can have a severe impact on both environment and society.

Natural groundwater fluctuations are a result of hydrometeorologic factors that are changing spatiotemporally, and topographic and hydrogeologic characteristics that are assumed to be temporally constant (e.g. Rinderer et al., 2019; Giese et al., 2020). The dominant hydro-meteorologic characteristic of cold humid (i.e. boreal, subarctic, snowy) climate zones are large quantities of winter precipitation, stored as snowpack in the cold months, and released as meltwater in spring (Clilverd et al., 2011; Jasechko et al., 2017). This seasonal snow cover highly affects the regional hydrology, e.g. discharge of rivers (Staudinger and Seibert, 2014; Jenicek et al., 2016; Dierauer et al.,

2018) or groundwater recharge (Kløve et al., 2017). Results from isotope analyses in central Canada indicate that snowmelt is the main source of annual groundwater recharge (Jasechko et al., 2017), which also explains why in Fennoscandia groundwater recharge generally reaches annual maxima during or after snow melting events (Kløve et al., 2017).

According to the climate scenario RCP8.5, cold humid climate zones are expected to go through a major shift northwards within this century (Rubel et al., 2017; Beck et al., 2018). The shift from cold to warmer, temperate climate is thus expected to influence the annual water budget in these regions (Clilverd et al., 2011; Jasechko et al., 2017). Whether the net effect on groundwater storage is positive or negative is unclear. A few studies already observe long-term consequences of seasonality changes and climate variability on groundwater levels. The general

trend is negative, coinciding with increased temperatures and precipitation, but overall results are highly variable (i.e. Allen et al., 2014). Two studies modelled the effect of rising temperatures on groundwater storage (Okkonen and Kløve, 2011) and recharge (Jyrkama and Sykes, 2007) in cold climate. Both studies state an increase of groundwater recharge in winter, as the change in dominating processes facilitate water infiltration and percolation through soil. This change in processes include (Jyrkama and Sykes, 2007; Okkonen and Kløve, 2011): [1] increased winter rain opposed to snowfall during a period with low to nil evapotranspiration, [2] decreased snow storage, which lead to reduced snowmelt magnitudes and a lower spring snowmelt peak, and [3] the reduction of soil frost that hinder percolation. Another modelling study by Sultana and Coulibaly (2011) claims that decreased snow storage (1 and 2) also leads to decreased annual groundwater recharge, although total annual precipitation increases. This could be related to changes in duration and intensity of precipitation events, as infiltration capacity varies with rainfall intensity (Fu et al., 2019). Nevertheless, it implies snow accumulation and melt processes facilitate recharge in general.

Lee et al. (2013) and Jang et al. (2015) studied the impact of climate on groundwater levels in a region with temperate and cold climate and a distinct wet season. They attribute the negative trend in groundwater levels to limited infiltration capacity. Therefore, increased precipitation in the wet season cannot contribute to increased recharge. Other studies predict that increasing precipitation will boost effective rainfall and groundwater recharge, overriding the increasing annual evapotranspiration rates with rising temperatures (Jyrkama and Sykes, 2007; Kovalevskii, 2007; Meixner et al., 2016).

However, shallow aquifers and aquifers with a thick capillary fringe are vulnerable as the hydraulic connection between root zone and aquifer enables vegetation to transpire and deplete groundwater (Kløve et al., 2014; Bloomfield et al., 2019; Condon et al., 2020). Unless balanced by sufficient rainfall, this would extend the duration of groundwater level recession and systematically reduce storage (Hamlet et al., 2007) such as presented in a catchment-scale modelling study for southern Finland by Luoma and Okkonen (2014). Other studies in cold humid (Scibek and Allen, 2006; Scibek et al., 2007) and also in cold to hot arid (Meixner et al., 2016) climate zones conclude that the effect of warming and increased precipitation on storage could be negligible. Thus, there remains a discrepancy in the interpretation of climate and seasonality effects on groundwater.

The overall objective of this study is therefore to improve the understanding of the connection between intra-annual fluctuations in hydraulic heads and hydrometeorological seasons specific to temperate and cold climate. Thus, the aim is to: [1] classify spatiotemporal differences in hydraulic head fluctuations, and compare to known climate zones; [2] elucidate spatial change in seasonality between two climatically different periods, and [3] quantify the effect of spatiotemporal change on hydraulic heads.

## 2. Study area and data

### 2.1. Climate

Sweden and Finland are located in northern Europe, between 55°–70° N and 10°–62° E. In this region, the climate zones range from temperate humid to cold humid with warm or cold summers (Fig. 1a). Based on the Köppen-Geiger climate classification (Kottek et al., 2006) cold climate is defined as having monthly average temperatures of more than 10 °C in summer but below –3 °C in winter. Temperate climate is defined as having monthly average temperatures also exceeding 10 °C in summer and between –3 °C and 18 °C in winter. Humid is defined as the climate lacking a dry season (Peel et al., 2007; Beck et al., 2018).

According to Chen and Chen (2013) climate zone classifications in Fennoscandia are highly unstable on inter-annual timescales. In northern Sweden and in Finland, the climate zones stabilise for decadal

to 30-year timescales. This is probably linked to the strong dependency to the Arctic Oscillation, North Atlantic Oscillation and Scandinavia teleconnections in winter, and to the East Atlantic/Western Russia teleconnections in spring and summer (Engström and Uvo, 2016; Irannezhad et al., 2019).

Regardless of climate zone classification, projections of average annual change according to the scenario RCP8.5 for the period 2011–2099, predict annual average differences in Sweden and Finland to be an increase in temperatures of ~ 0.06 °C, and in precipitation of ~ 0.25% (SMHI, no date; Ruosteenoja et al., 2016).

### 2.2. Hydrogeological context

The hydrogeological context is important to reduce misconceptions and misinterpretations of the results, even though it is not the focus of the study. Nordic hydrogeology is different in terms of typical mechanisms and processes that prevail in central or southern Europe. In general, aquifers in sedimentary formations are limited in depth and spatial extent, resulting in local aquifers (Asch, 2003). These small aquifers often lack a connection to rivers and streams, as low-permeability bedrock isolate sedimentary deposits. Thus, the mechanisms of groundwater-surface water interactions often differ from those in other parts of the world. The geology and landscape is strongly influenced by peneplanation and recent glacial history, and thus very different from regions that have not undergone these processes. For example, the vadose zone is generally thin, so the mostly unconfined shallow groundwater systems are well-connected to the atmosphere (Richts et al., 2011; Fan et al., 2013).

The bedrock in Sweden and Finland is part of the Fennoscandian Shield, a geologically distinct area of the European Craton. The bedrock is mainly composed of granites and gneisses from the Archaean and Proterozoic eons with relatively few and small elements of (mostly) Palaeozoic lime- and sandstone (Fig. 1b) (Adrielson et al., 2006; Fredén, 2009). Due to long-term peneplanation, the bedrock surface and surface topography is mostly flat or gently undulating (Lidmar-Bergström et al., 2013). Bedrock and superficial sedimentary deposits are separated by an unconformity, shaped by Quaternary glacial erosion. This together with earlier peneplanation and glacial deposition has created a knock-and-lochan landscape (shield terrain), with surficial layers mainly consisting of till (Kleman et al., 2008; Ebert et al., 2015). The diagenesis and permeability of the glacial deposits is affected by different stages of the Baltic Sea, which is delimited by the elevation of the highest shoreline (Åberg, 2013; SGU, 2015). The highest shoreline elevation varies between 10 and 289 m.a.s.l. and 20–109 m.a.s.l. in Sweden and Finland respectively. Below the highest shoreline, sediments have a subaquatic origin and are therefore more well-sorted and have extensive silt and clay lenses. Above the highest shoreline sediments have a supra-aquatic origin. These layers are hence heterogenous and unsorted. Supra-aquatic till is often clayey resulting in a low hydraulic conductivity (Englund et al., 1986). Regionally, depth to bedrock is commonly < 10 m (Kleman et al., 2008). Exceptions are fracture valleys, eskers and end-moraine formations (see Fig. 1b, coarse sediments) where thicknesses of more than 100 m can be reached (Fredén, 2009; Stroeven et al., 2016; Ymparisto, 2019). The piezometers used in this study are all located in superficial glacial deposits of subaquatic or supra-aquatic origin.

### 2.3. Data

#### 2.3.1. Climate data

The Finnish Meteorological Institute (FMI) provide data of daily sums of precipitation and average temperatures for Finland. The dataset is part of FMI ClimGrid, a 100 km<sup>2</sup> daily regional reanalysis climate grid covering the period 1961–2014 (Aalto et al., 2016). The Swedish Meteorological and Hydrological Institute (SMHI) provide data of daily sums of precipitation and average temperatures for Sweden. The

dataset is part of the regional reanalysis for Europe, a Copernicus Climate Change Service (Undén, 2017). It is a 121 km<sup>2</sup> daily regional reanalysis climate grid covering the period 1961–2015.

### 2.3.2. Groundwater data

Groundwater hydrographs are provided by the Swedish Geological Survey (SGU) and the Finnish Environment Agency (SYKE). The time series contain at least 31 years of biweekly observations (1980–2010), with a maximum of 4 months missing data. Missing data is imputed by the mean of the previous and following measurement. Piezometers with data classified as having bad quality by SGU or SYKE, and time series visually affected by unnatural disturbances, are excluded. Groups where piezometer hydrographs have highly variable fluctuation are excluded from further analysis, as this is likely due to anthropogenic influence.

After pre-processing, 264 piezometers (74 geographically distinct groups), out of ~1500 piezometers (197 groups) remained, with bi-weekly (on average 1.8 measurements/month) observation intervals. The distribution of piezometers per geographically distinct group (1–11, median of 5) is detailed in Table A.1. The piezometers used in this study are all in glacial sediment at a surface elevation lower than 500 m.a.s.l., with a median depth below surface ranging between 0 to 18 m (Fig. 2).

## 3. Methods

### 3.1. Classification of hydrometeorology

The classification of hydrometeorology is based on a simplified water budget for each climate grid cell:

$$P = ET + Q + \Delta S \quad (1)$$

where P [mm] is precipitation, ET [mm] is evapotranspiration, Q [mm] is stream discharge, and  $\Delta S$  [mm] is dynamic groundwater storage (the net effect of groundwater recharge and discharge).

Since ET is unknown, potential evapotranspiration (PET) is used as an approximation. Mean monthly PET [mm] is calculated using the SPEI package in R Studio (Beguería and Vicente-Serrano, 2017) based on Thornthwaite (1948) as

$$PET_m = 1.6N_m \left( \frac{10T_m}{I} \right)^a \quad (2)$$

With

$$I = \sum \left( \frac{T_m}{5} \right)^{1.514} \quad (3)$$

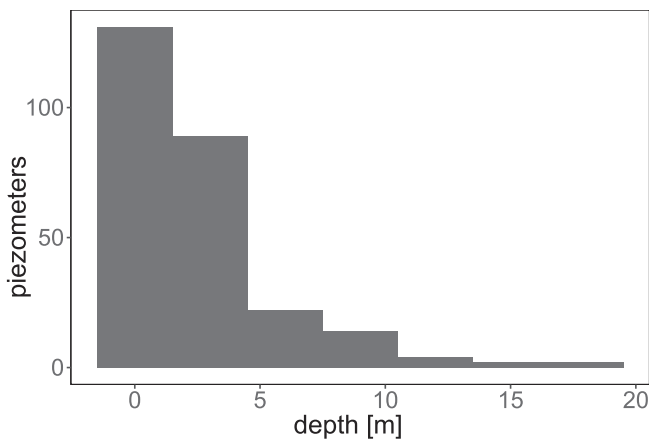


Fig. 2. Histogram of median depth to groundwater, for the 264 piezometers used in the study and the years 1980–2010.

$$a = 6.75 * 10^{-7} * I^3 - 7.71 * 10^{-5} * I^2 + 1.791 * 10^{-2} * I + 0.49239 \quad (4)$$

where m is the month, N [–] is a factor based on latitude and month that accounts for daylight hours. Latitudes above 50° N have the same correction factor (i.e. all piezometers in the study). T [°C] is the mean monthly temperature and I [–] is the heat index.

The relationship between mean monthly temperatures and PET is highly complex. The complexity increases in warmer climates and decreases in colder climates. The approach does not account for freezing temperatures and differences in land cover, which affect PET. Thornthwaite (1948) acknowledges that the relationship differs based on location, and PET tends to be overestimated, especially in tropical or warm climates. However, the method is preferable due to the small data requirements and the expected small errors in the cold and temperate climate zones of Fennoscandia. Variations in evapotranspiration due to varying plant properties and land use change are not considered, as no vegetation data is included in the approach.

Since the study is focussed on  $\Delta S$  as a function of water availability, i.e. P–ET, and due to the generally low hydraulic connection between rivers and aquifers, the groundwater component of Q is considered constant as a simplification. Effective precipitation (P–ET) determines surface water availability for infiltration and percolation, and  $\Delta S$  indicates the effect on groundwater. Surface water surpluses or deficits, as determined by effective precipitation, are represented by two hydrometeorology types (“rain” and “high PET” respectively).

For every hydrometeorological type and the assumption that base-flow is constant, drivers of dynamic groundwater storage can be written as

$$\Delta S = RS - ET \quad (5)$$

where RS [mm] is the rainfall and snowmelt output from the snowmelt model. In temperate and cold climate, a surface water surplus facilitating infiltration mainly occurs when rainfall or snowmelt production exceeds PET, these types will hereafter be referred to as ‘rain’ or ‘snowmelt’. Surface water deficits, or weakening of infiltration, occurs when PET exceeds rainfall, this is referred to as ‘high PET’ in the classification (Jasechko et al., 2014), or when precipitation accumulates as snow at the surface, hereafter referred to as ‘snowfall’ (Clilverd et al., 2011; Jasechko et al., 2017). If there is snowfall, effective precipitation (RS–ET) is 0 mm. The classification according to Eq. (5) is applied to each re-analysis climate grid cell, and is based on daily average values of RS, PET, and melt production (M, Eq. (8)) for two different periods (see Section 4.1 Climate context for a description of the two periods chosen for analysis).

For the classification of hydrometeorology as ‘snowmelt’, evapotranspiration and rain are excluded to emphasise the effect of snowmelt on hydraulic head dynamics. The hydrometeorology is given the ‘snowmelt’ classification when snowmelt production exceeds 0.5 mm (Table 1). This is due to the computation of 10-year means producing low values of daily snowmelt, meaning a threshold of 0 mm snowmelt greatly exaggerates average snowmelt days. Rain-on-snow episodes are not represented. Each condition is specified in Table 1.

#### 3.1.1. Precipitation phase

To calculate the sums of daily snow water equivalent and snowmelt, a single temperature index-based model is used. The method is based on

Table 1  
Condition for each hydrometeorology type classification.

Hydrometeorology type	condition
high PET	PET > RS
snowfall	RS = 0 = PET
rain	PET < RS
snowmelt	M > 0.5 mm

the snow routine of the HBV model, using five coefficients describing empirical relationships between water freezing, melting and snowpack runoff (Bergström, 1976). The approach may be simplified as

$$P = P_S \text{ when } T < 1^\circ\text{C} \quad (6)$$

$$P = P_L \text{ when } T > 1^\circ\text{C} \quad (7)$$

where  $P_S$  [mm] is solid precipitation i.e. snow water equivalent and  $P_L$  [mm] is liquid precipitation i.e. rain. Snowmelt production ( $M$ ) is simulated according to a degree-day factor (how much snow may melt per degree per day) regardless of precipitation, as

$$M = \min(A, C_M * (T - TT)) \quad (8)$$

where  $A$  [mm] is snowfall accumulation of the previous day,  $C_M$  [2.74 mm/°C/day] is the degree-day factor,  $T$  [°C] is the air temperature and  $TT$  [°C] is the air temperature threshold. A detailed account of the different steps are described in [appendix B](#). Literature parameter values optimised for Sweden are used for the entire study area (Seibert, 2005; Seibert and Vis, 2012). A temperature threshold of 1 °C is used for the study based on findings from Feiccabrino and Lundberg (2008).

### 3.2. Classification of groundwater hydrographs

This study aims to elucidate the relationship between dynamic groundwater storage and varying groundwater recharge. The approach considers fluctuating hydraulic heads and recharge as a product of infiltration and percolation of effective precipitation (Eq. (5)).

Because discharge (as a product of runoff, subsurface flow and groundwater drainage), and hydrogeological properties of the piezometer locations are unknown, dynamic storage ( $\Delta S$ ) cannot be directly quantified. However, temporal variation of  $\Delta S$  is represented in relative terms by fluctuations in hydraulic heads. This fluctuation represents a relationship that, based on a simplified aquifer water budget, can be written as

$$\Delta S = G_R - G_Q \quad (9)$$

where  $G_R$  [mm] is groundwater recharge, and  $G_Q$  [mm] is groundwater discharge. For natural hydrogeological systems undisturbed by human influence, rising hydraulic heads (RH) corresponds to  $\Delta S > 0$  i.e.  $G_R > G_Q$ , and declining hydraulic heads (DH) corresponds to  $\Delta S < 0$  i.e.  $G_R < G_Q$ . Identifying RH and DH patterns enables the analysis of piezometric hydrographs for the qualitative determination of timing and duration of fluctuating patterns in hydraulic heads. By connecting RH and DH to hydrometeorology types, inferences on the impact of different hydrometeorology on dynamic groundwater storage in cold and temperate climate can be made.

A statistical approach is applied to quantify differences in hydraulic heads for all piezometers, using measures of depth to groundwater. Depth to groundwater is estimated by subtracting the surface elevation by hydraulic heads and dividing the result by the record median head. Thereby, values are made dimensionless and spatially comparable. For each period and piezometer, this value is used to calculate measures of the seasonal standard deviation of, median, minimum and maximum depth(s) to groundwater. The standard deviation indicates inter-annual differences. The median indicates median groundwater depth per season (winter: DJF; spring: MAM; summer: JJA; autumn: SON) and period. Minimum and maximum values indicate lowest and highest depth to groundwater attained per season and period. The percent difference between the two periods, for every measure and piezometer, is calculated. The result is presented as the median of the percent difference for each latitude group, defined based on the climate zones in [Fig. 1a](#), together with the significance. The significance is tested using

the paired nonparametric (two-tailed) Wilcoxon Signed-Rank test (Bauer, 1972). A paired test is used since the measures are affected by the fluctuation amplitude of hydraulic heads, which are spatially heterogeneous and specific to hydrogeological characteristics.

Measure results per piezometers are plotted and analysed one period against another to visualise differences. This enables the relative quantification of local changes, presumably caused by differences in climate.

### 3.3. Linking hydraulic head fluctuations to hydrometeorology

To simplify the spatial component of the analysis, piezometers are grouped by proximity. Piezometers are grouped according to their location in the climate grid cell (100 km<sup>2</sup> for Finland, 121 km<sup>2</sup> for Sweden). Most piezometers within the same group (i.e. climate grid cell) portray similar seasonality. Some piezometers are apparently different in dynamics within the group (e.g. slope, amplitude). This can be due to strong local differences in hydrogeology or even the location in different aquifer systems. However, since the analyses on groups focus on differences in timing of fluctuations (initiation/duration of RH or DH), it is not considered detrimental to the study that groups may have piezometer hydrographs with different shape such as slope, recession curve, and amplitude in fluctuation (see [appendix C](#) for all median hydraulic heads of individual piezometers in all groups).

For the analysis of groups, the hydraulic heads of each piezometer are first normalised by subtracting the surface elevation and median period hydraulic head. To get the normalised head per group, the median of heads within each group is calculated for each biweekly time step. Hydraulic head fluctuations at smaller temporal resolution are not retained. However, for the comparison to hydrometeorology, fluctuation patterns are interpolated between observations to a daily resolution.

Hydraulic head and hydrometeorology classifications are linked as follows. The day-of-year with a specific hydrometeorology is associated to the same day-of-year hydraulic head class (rising or declining heads). Each piezometer class-hydrometeorology pair is presented per period and season. Days with a specific pair are summarised per season, and the duration for such a relationship, e.g. rising heads associated with rain, are presented as a fraction of that season, e.g. Sep–Nov.

## 4. Results

### 4.1. Climate context

To put the study in a climate change context, annual, decadal and 15-year means of temperature and precipitation are calculated for the three climate zones ([Fig. 1](#)) between 1980 and 2010. This indicates generally increasing temperatures between 1980 and 2010 ([Fig. 3](#)). Annual sums of precipitation is mainly increasing for the temperate and cold climate zone and decreasing for the cold climate subcategory of ‘warm summers’, referred to as the climate transition zone ([Fig. 1](#), ~59°–63° N). The 1990’s show opposing trends in precipitation for the temperate and the cold (latitudes above 63° N) climate zones, compared to the general trend between 1980 and 2010.

Projected changes for Sweden and Finland are based on model ensemble results for the scenario RCP8.5, covering the period 2000–2099 and 2000–2084, respectively. The average annual increase for the projected changes and their corresponding period is 0.05–0.07 °C per year for temperature and 0.2–0.3% per year for precipitation. For a 20-year period, which correspond to differences between the middle of the 1980’s and 2000’s, the increase is 1.0–1.4 °C and 4.3–6.4% (SMHI, no date; Ruosteenoja et al., 2016). This is similar to differences between

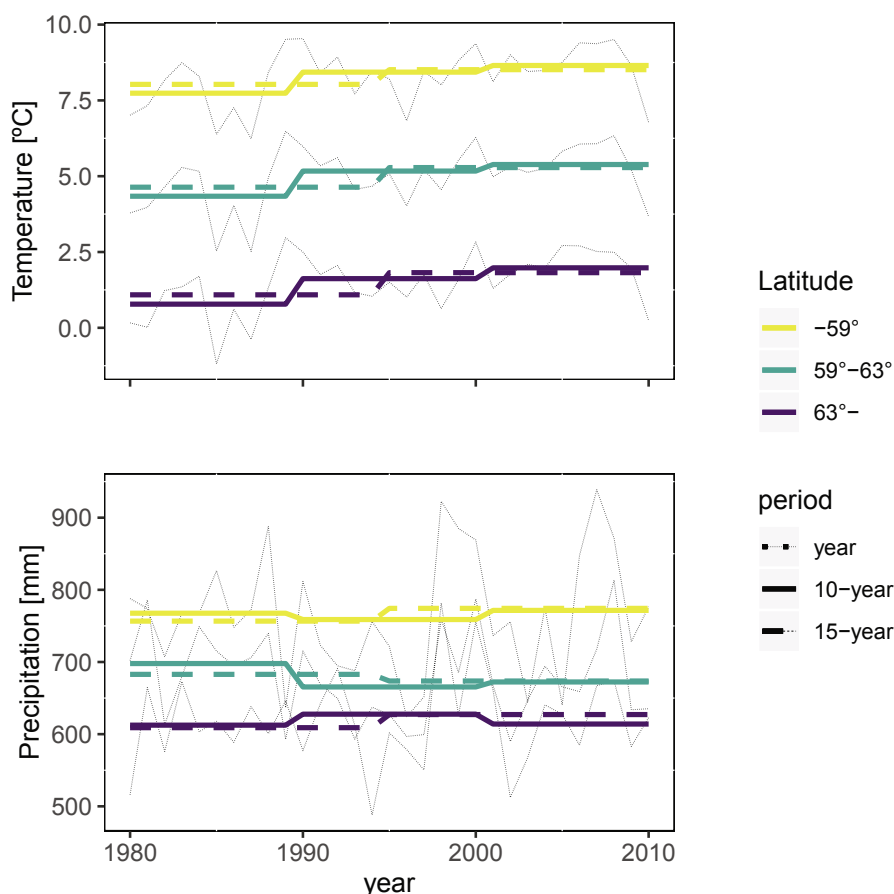


Fig. 3. Mean annual, decadal and 15-year means of average temperature and sums of precipitation per three latitude groups defined according to climate zones in Fig. 1a.

the 1980's and the 2000's, with a mean annual temperature and precipitation difference of 0.9–1.2 °C and –4–1.8%, respectively (Fig. 3). Therefore, to match general precipitation trends and maximise the difference in average temperature between the two periods, the data is divided and analysed using two 10-year periods: 1980–1989 (P1) and 2001–2010 (P2).

#### 4.2. Seasonality of the hydrologic cycle

In general, seasonality in groundwater fluctuation follow a distinct pattern in Fennoscandia as presented by four piezometers in Fig. 4. In cold climate (piezometer 23 and 1204p10), heads rise quickly as temperatures increase above the freezing point in spring. Thereafter, heads either remain high during summer (1204p10), or decrease if temperatures are warm (23). If heads decline during warm conditions, they rise again as temperatures decrease in autumn. As temperatures drop below the freezing point in winter, hydraulic heads continuously decline until temperatures rise again in spring. This general trend occurs regardless of the amount of precipitation, except in summer during sustained precipitation over more than a few days.

In temperate climate (piezometer 9 and 3, Fig. 4), temperatures usually are not below the freezing point for long. Thus, in winter, hydraulic heads rise. Summers are warmer, and hydraulic heads decline. The declining trend usually continues until temperatures decrease in autumn.

#### 4.3. Classification of hydrometeorology and groundwater hydrographs

The results from the hydrometeorology and hydrograph classifications for 8 groups are shown as examples from P1 and P2 in Fig. 5 (the annotated groups in Fig. 1a). There is a clear geographical distinction, with group 1 being northernmost and 8 the southernmost group (Fig. 1a). The northern groups (1–4) have a distinct snowfall period with DH and spring snowmelt peaks, with some (2–4) also having a summer recession during high PET. The southern groups (5–8) have a long summer recession, but generally RH in autumn and winter during rainfall. Group 5–7 also have a short winter recession followed by an increase with spring snowmelt (similar to groups 1–4).

Between P1 and P2 the groundwater fluctuations are different either in timing, duration and/or amplitude (Fig. 5). For example, group 2 has a change in timing and amplitude of groundwater fluctuations, with a slightly longer autumn recession. Another example is group 4, which has a shorter winter recession and a longer summer recession, and also a different amplitude in fluctuations. Simultaneously, the snowfall period has a shorter duration in P2 than in P1, intermixed with days of snowmelt, rain and high PET (groups 2–5). There is an increase in high PET (groups 1–5), and in rain duration (3–5).

#### 4.4. Quantitative difference in hydraulic heads

The comparison of hydraulic heads indicate that changes to groundwater storage have occurred between P1 and P2. Fig. 6 shows

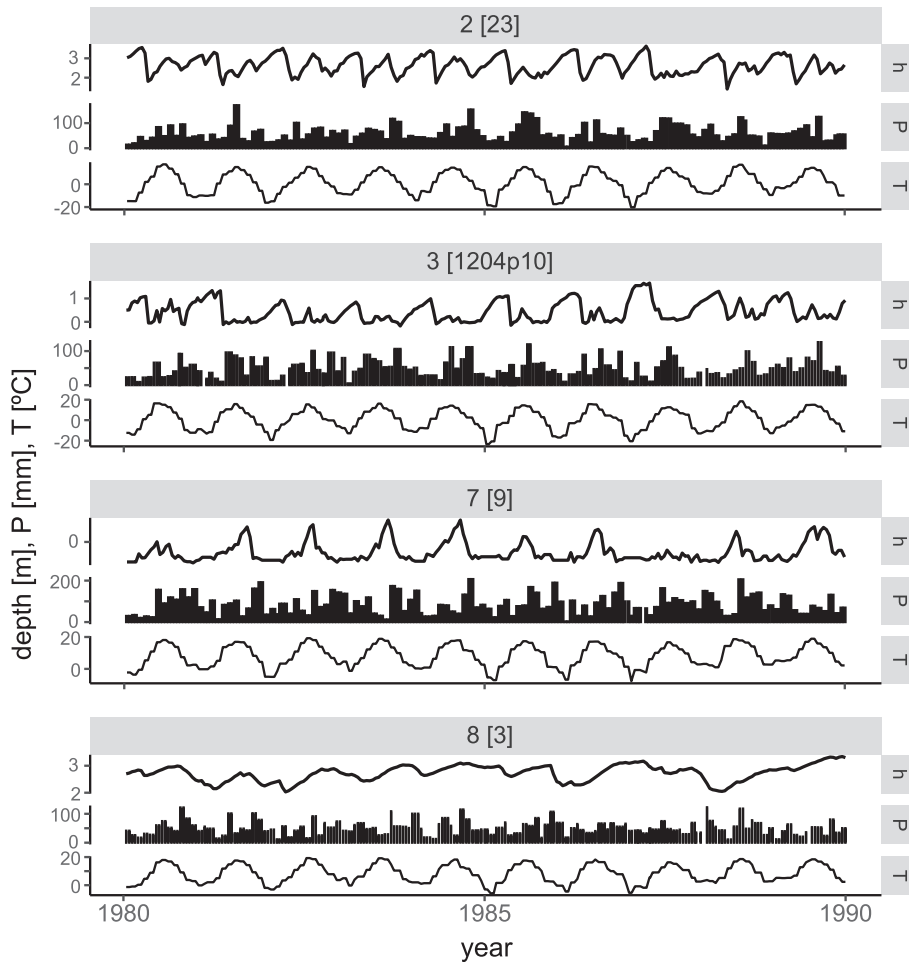


Fig. 4. Biweekly observations of depth to groundwater (h), sums of precipitation (P) and average monthly temperature (T) data from four piezometers used in the study, and their corresponding climate grid cell. Labelling refers to the piezometer group number, and the piezometer id in square brackets.

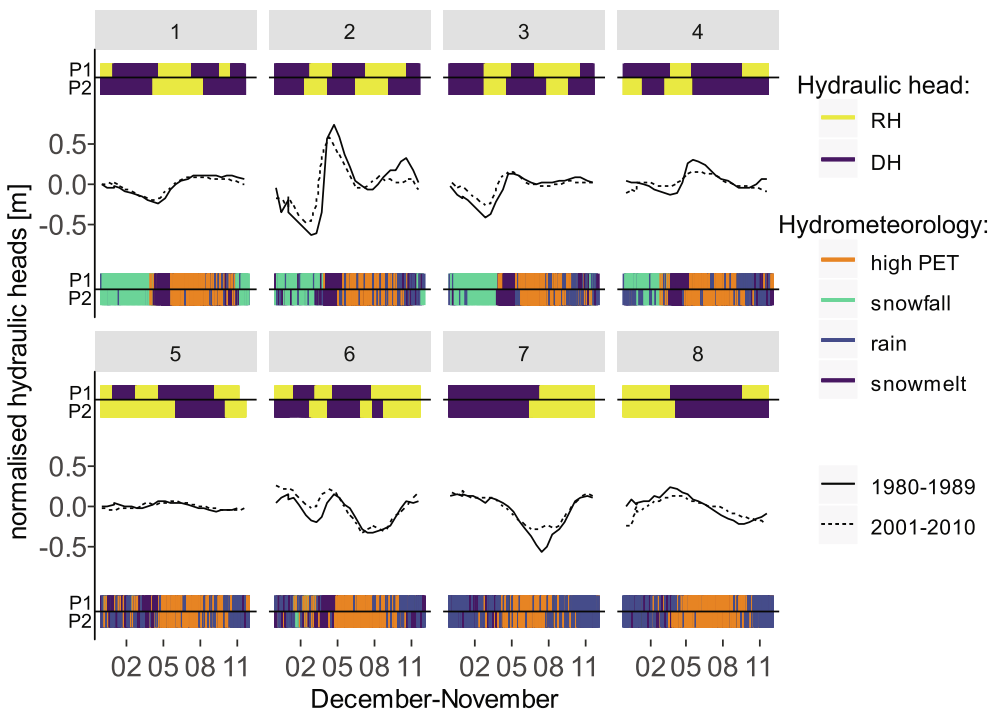
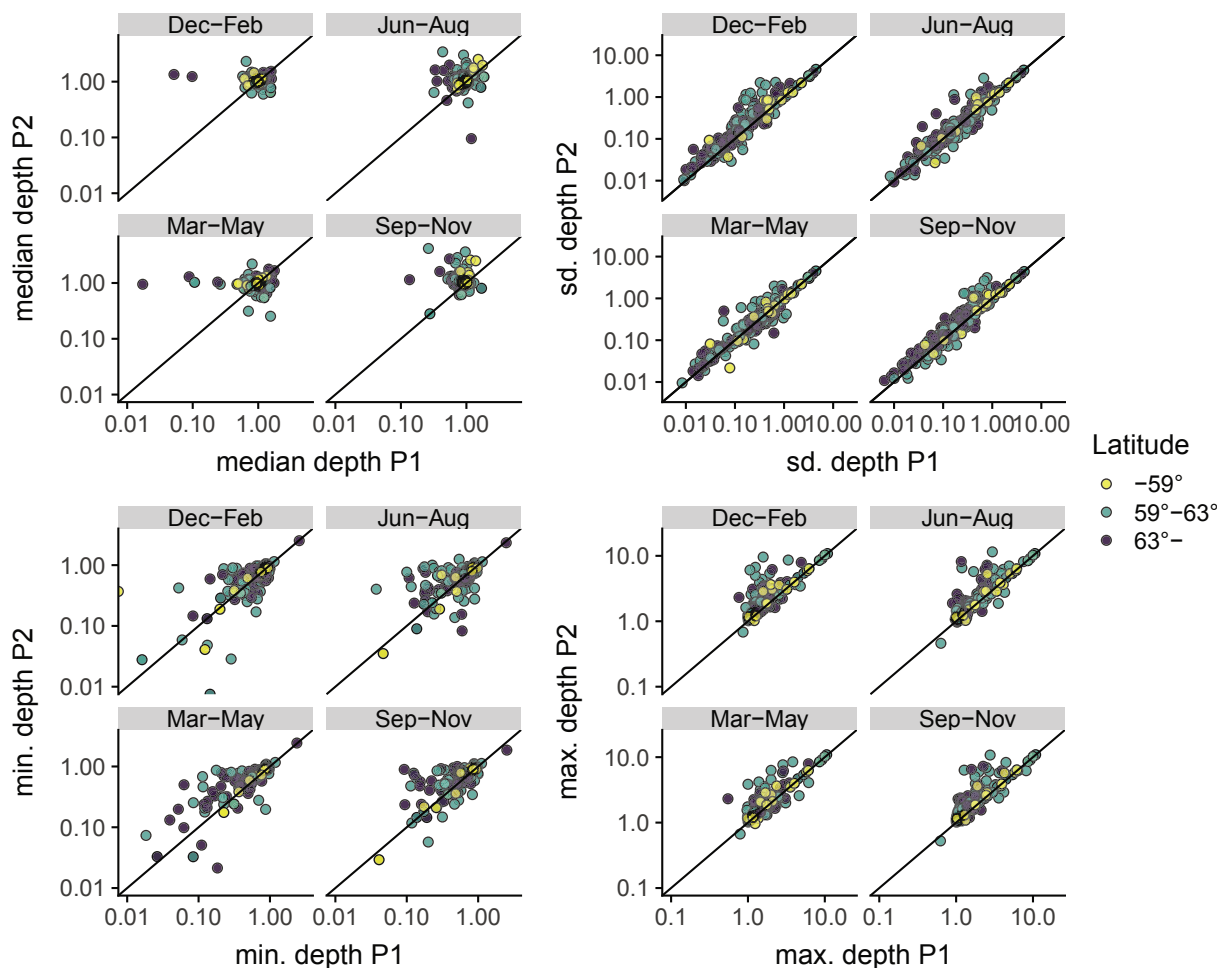


Fig. 5. Daily hydrometeorology and groundwater classifications plotted with the normalised hydraulic head fluctuations for 8 selected groups annotated in Fig. 1a. The groundwater classification is shown as columns per day at the top of the plots (RH vs. DH), and the hydrometeorology types at the bottom. P1 = 1980–1989, P2 = 2001–2010. RH = rising hydraulic heads, DH = declining hydraulic heads. Month ticks marks the beginning of each month. Results from all groups are in [appendix D](#).



**Fig. 6.** Measures of median, minimum (min.), maximum (max.) and standard deviation (sd.) of depth to groundwater per piezometer. The black line indicate where values for 1980–1989 (P1) and 2001–2010 (P2) are identical.

**Table 2**

Percent difference between 1980–1989 (P1) and 2001–2010 (P2) for each latitude group (corresponding to the climate zones, Fig. 1a), based on Fig. 7. Measures stand for the standard deviation of (sd.), median, minimum (min.) and maximum (max.) depth to groundwater. A positive percent difference indicates an increase in depth to groundwater, i.e. decreased groundwater storage in P2 vs. P1, and vice versa. No star = p-value not significant. \* = p-value < 0.05. \*\* = p-value < 0.01. \*\*\* = p-value < 0.001.

Season	Latitude	median	sd.	min.	max.
				%	
Dec-Feb		3*	3	1	2***
Mar-May		7**	1	4	3**
Jun-Aug	-59°	5*	1	-25	2
Sep-Nov		7***	1	-19	2**
Dec-Feb		4***	10***	4	6***
Mar-May		4*	3	9**	5***
Jun-Aug	59°-63°	5***	1	8***	4***
Sep-Nov		10***	1*	8***	4***
Dec-Feb		3***	23***	1	5***
Mar-May		-1	0	7***	4***
Jun-Aug	63°-	6***	5*	1*	6***
Sep-Nov		9***	20***	5***	7***

the hydraulic head changes expressed as depth to groundwater for each piezometer and period, and in Table 2 the difference is summarised by the median percent difference for each latitude group/climate zone.

Most piezometers have increased depths to groundwater in P2 compared to P1 (Fig. 6), and this is clearly mirrored by the percent difference (Table 2). The magnitude of the difference varies by season, both for individual piezometers (Fig. 6) and collectively for the three latitude groups/climate zones (Table 2).

The minimum depth to groundwater represents high-level conditions in the piezometers. Based on the hydrologic seasonality (Fig. 4), piezometers in cold (temperate) climate normally have high-level conditions in spring (winter). However, for the latitudes 59°–63° N and north of 63° N, the spring minimum depth has increased more than in any other season in P2. The minimum depth is higher in summer and autumn as well, with no significant change in winter. There is no significant change in minima south of 59° N (Table 2).

Changes in autumn and winter, seasons which represent the end and the beginning of the hydrologic year, indicate accumulated differences in storage throughout the year. For the latitudes 59°–63° N and north of 63° N, the autumn or winter change in median and maximum depth is the largest between the seasons, and is significantly deeper in P2 than in P1 (Table 2). Furthermore, the standard deviation, indicating changes

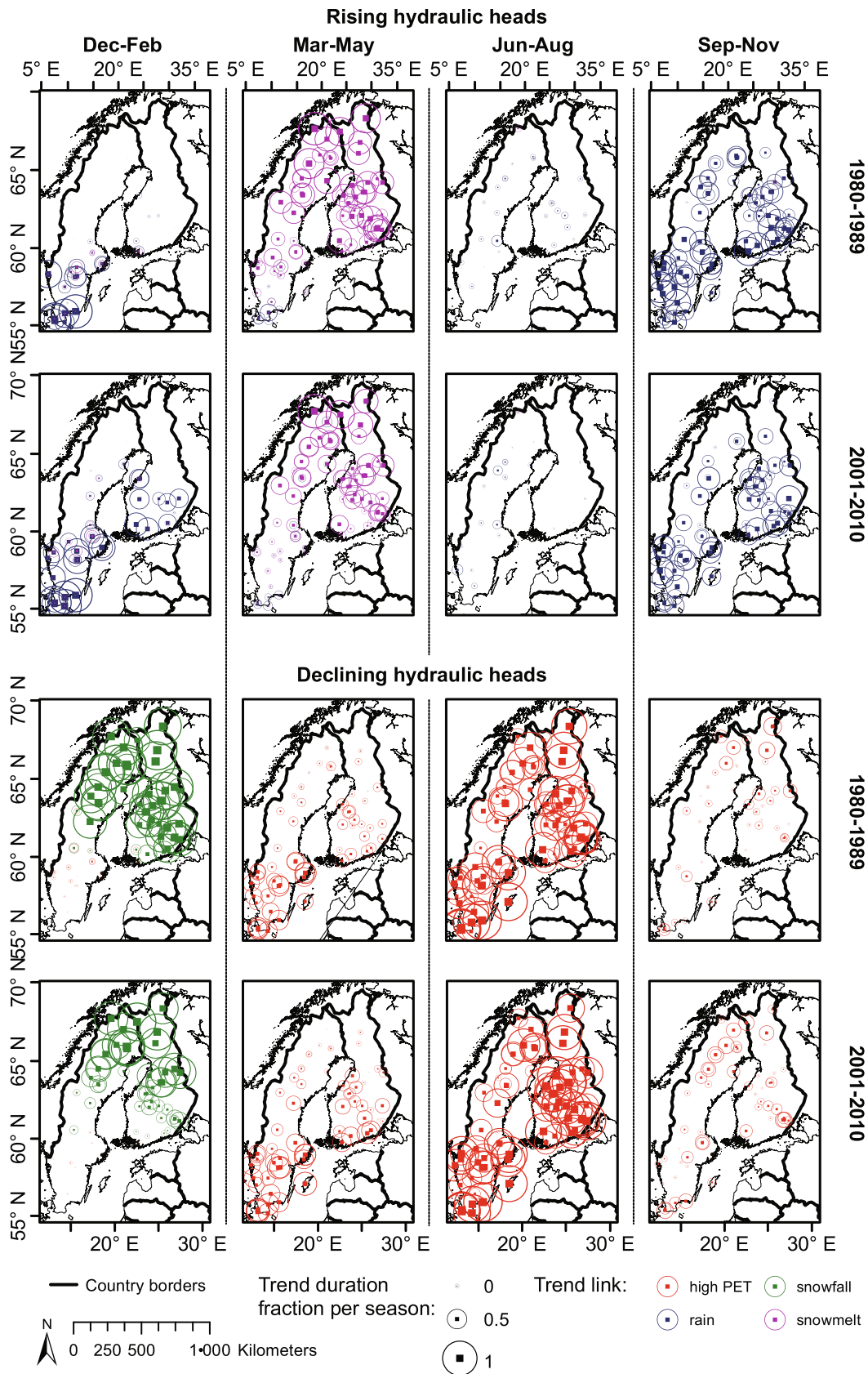
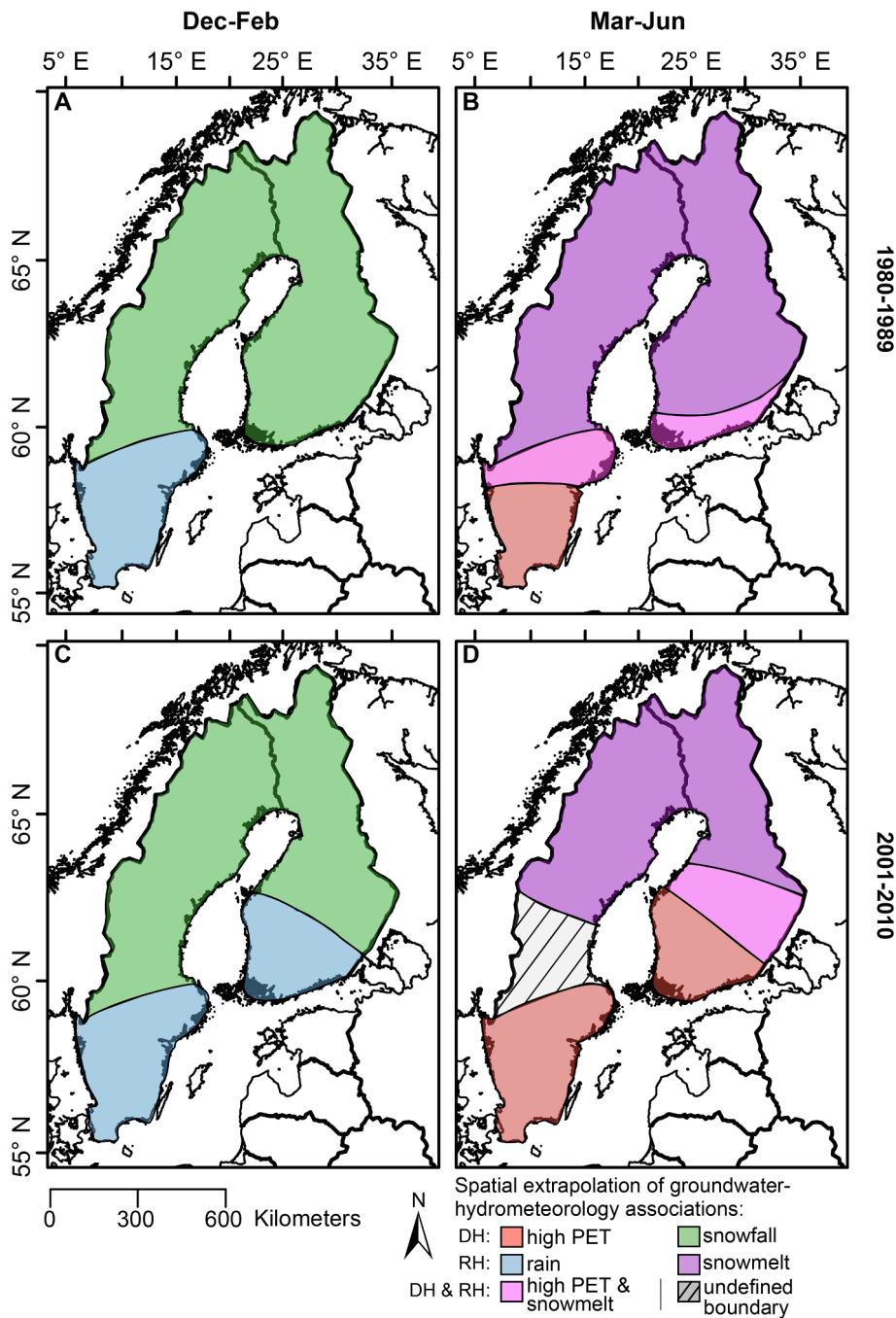


Fig. 7. Each circle corresponds to one group of piezometers. Their size define the fraction per season (duration) with a specific groundwater-hydrometeorology association. The colour of the circle specifies the hydrometeorology type. Country borders are based on EuroGraphics and UN-FAO, @EuroGraphics. All groundwater-hydrometeorology associations realised are in [appendix E](#).



**Fig. 8.** Conceptual inter- and extrapolation of the spatiotemporal extent of groundwater-hydrometeorology association based on Fig. 7. In green are areas where groups have DH associated to snowfall, in blue where they had RH associated to rain (A and C). B and D show areas where RH occur in association to snowmelt (purple), and DH in association to high PET (red). The pink colour indicates piezometer groups where hydraulic heads were both rising and declining in association to the different hydrometeorology types in spring.

between P1 and P2 of the inter-annual variability within the two decades, is significantly higher at 10% and 23% difference in winter at 59°–63° N and north of 63° N, respectively. This implies that there is an increased variability in storage at the beginning of the hydrologic year in P2. The standard deviation south of 59° N has not changed significantly, but autumn median depths have the highest significant percent difference (a 7% increase in depth) from any of the measures and seasons. Thus, piezometers at all latitudes have, generally,

significantly decreased groundwater storage in P2 (Table 2). However, it should be noted that there is also large variability between piezometers, and some have decreased depths to groundwater, i.e. increased storage, in P2 compared to P1 (Fig. 6).

#### 4.5. Link between hydraulic head fluctuations and hydrometeorology

Seasonality in groundwater is mainly characterised by RH in spring

and autumn, and DH in winter and summer. There is a spatial boundary around 60° N (Fig. 7). In winter, DH dominates north of 60° N (Finland and northern Sweden), and is associated with snowfall. South of 60° N (southern Sweden) RH is predominant in winter and is associated with snowmelt and rain. Spring is characterised by snowmelt and RH throughout Fennoscandia (Fig. 7). Although southern Sweden is affected by DH associated to high PET in spring as well. Days classified as rain occur throughout the year, but are most frequent in autumn and spring in association with RH, particularly southward. In summer, high PET conditions dominate in association with DH. Thus, spatial differences in hydrometeorology type association to hydraulic head pattern is most apparent in winter and spring.

Between the two periods, there is a spatiotemporal change in groundwater-hydrometeorology links. In winter, RH associated with rain has migrated north in P2, occurring south of ~62° N (Fig. 7). In spring, the same groups have a shorter RH duration. High PET-associated DH has increased in occurrence and duration in the entire study area. This increase is most pronounced during spring in southern Sweden and Finland. The duration of snowfall-associated DH at latitudes south of ~65° N have shortened or ceased. There appears to be fewer days with a RH pattern in autumn (P2) overall, but in northern Sweden in particular.

## 5. Discussion

### 5.1. Spatiotemporal differences in hydraulic head fluctuations

The approach of associating rising or declining hydraulic heads with hydrometeorology indicates the spatial and temporal differences in the two climate zones (cold and temperate, Figs. 1a and 8). In accordance with studies on groundwater recharge in temperate climate (Lee et al., 2013; Jasechko et al., 2014; Jang et al., 2015), southern Sweden has a long duration of rising hydraulic heads associated with rain in winter, and declining hydraulic heads associated with high evapotranspiration in spring (Fig. 8). Northern Sweden and Finland have a long duration of declining hydraulic heads associated with snowfall in winter, and rising hydraulic heads associated with snowmelt in spring. This is consistent with findings from other studies in cold climate regions, regarding the effect of these hydrometeorological conditions on groundwater recharge and, consequently, storage (Jyrkama and Sykes, 2007; Clilverd et al., 2011; Okkonen and Kløve, 2011; Luoma and Okkonen, 2014; Jasechko et al., 2014, 2017).

In summer and autumn the spatial differences are less pronounced. Generally in the study area, declining hydraulic heads associated with high evapotranspiration occur in summer, while rising heads associated with rain occur in autumn (Fig. 7). Consequently, rain and evapotranspiration affects hydraulic heads in both climates.

### 5.2. Spatial changes in seasonality between P1 and P2

In addition to spatial and seasonal differences, there is a notable difference in the spatial extent of different seasonal characteristics between the two periods P1 (1980–1989) and P2 (2001–2010), particularly above the temperate-cold climate zone boundary (~59° N, Fig. 1a). Differences are most apparent in winter and spring (Fig. 7, conceptualised in Fig. 8). Temperate zone conditions have shifted north in P2. The duration of rising hydraulic heads, associated with rain in winter, have migrated northeast, and snowfall associated with declining heads have retracted. In spring, the duration of rising heads associated with snowmelt has decreased and retracted similarly to the snowfall pattern in winter. High evapotranspiration associated with declining heads occurs in Sweden south of 60° N, and in Finland south of 64° N (Fig. 7). The spatial difference between P1 and P2 is not as clear in

Sweden as in Finland. However, data quality requirements lead to a low number of piezometers in Sweden at these latitudes. Thus, the absence of a visible change is not conclusive. Nevertheless, GCM results for 1901–2100, based on an ensemble of IPCC scenarios, indicate that the climate zone shift in Sweden is delayed compared to same-latitude shifts in Finland (Rubel and Kotteck, 2010). This may explain the lack of visible spatial change between P1 and P2 in Sweden.

### 5.3. Impact on hydraulic heads

A cold-to-temperate climate shift would make groundwater increasingly affected by rain and evapotranspiration and less by snow processes, as temperatures increase and land cover evolves (Sultana and Coulibaly, 2011; Scheliga et al., 2018; Wang et al., 2018). Most studies agree that this leads to increased winter infiltration and summer evapotranspiration (e.g. Jasechko et al., 2014). Therefore, the seasonality of precipitation is considered a key feature of annual groundwater recharge (Clilverd et al., 2011; Okkonen and Kløve, 2011; Jasechko et al., 2014). The changing seasonality of hydrometeorology may here be defined as [1] the transition from snowfall-dominated to rainy winters, and [2] high evapotranspiration in spring, previously dominated by snowmelt.

The percent difference in depth to groundwater (Table 2) clearly show that depths are significantly deeper in P2 compared to P1, in all seasons. This suggests that recharge in P2 cannot maintain the groundwater storage of P1. Therefore, in contrast to modelling studies which found [1] and [2] leading to increased groundwater recharge in the future (e.g. Jyrkama and Sykes, 2007; Kovalevskii, 2007; Clilverd et al., 2011), the here presented results suggest the opposite. This, despite the general trend of increasing precipitation in most of the region (Fig. 3). Piezometers north of 59° N show a larger variability from the group median (Fig. 6), indicating the change is largest in the location of most seasonal change. This could be related to changes in precipitation patterns, as not only total amounts but also the intensity of precipitation affects infiltration and percolation processes (Clilverd et al., 2011). Furthermore, some studies argue that, depending on the growing season, effective recharge from rainfall could decrease in relation to snowmelt (Clilverd et al., 2011; Hamlet et al., 2007; Hinzman et al., 2005).

Significantly deeper autumn and winter depths, including the increase in standard deviation, indicate that increasing groundwater depths are inherited by successive years (Table 2). Consequently, groundwater storage decreases continuously on an inter-annual perspective, despite increased duration of rising hydraulic heads in winter. Although less self-evident, this implies antecedent conditions are indeed hugely important for the water balance, as found by Okkonen and Kløve (2011), Van Loon (2015), Dierauer et al. (2018) and Cuthbert et al. (2019).

Some piezometers have decreased depths, i.e. increased storage, in P2 compared to P1 (Fig. 6). Scibek and Allen (2006), Allen et al. (2014) and Meixner et al. (2016) report divergence from large scale trends or ambiguity in results, which they attribute to hydrogeological limitations or complexity. Additionally, differing forest canopy cover has been modelled to greatly alter recharge (Ala-aho et al., 2015). Thus, land cover and land use change, in addition to hydrogeology, has the capacity to greatly affect groundwater recharge and influence the net effect of a climate shift. It is not possible to derive the cause of variability in the change of depth to groundwater in this study. However, it is likely that heterogeneity of hydrogeology and differences in land cover is causing variance in the response to changing climate pressures.

#### 5.4. Implications of shifting cold climate zones for changing groundwater seasonality on the global scale

Compared to studies on groundwater resources in a global context, where focus is on regional aquifers in extensive sedimentary deposits, hydrogeology in Sweden and Finland is dominated by small aquifers with relatively low hydraulic connectivity. Groundwater resources in much of the northern hemisphere, north of 50° N, has been similarly classified (Richts et al., 2011; Fan et al., 2013). Additionally, the unsaturated zone is commonly very thin (< 2 m), and water tables are well-connected to the atmosphere. This results in little capacity of the groundwater system to buffer climate change over more than a few years (Cuthbert et al., 2019). Considering that temperature and precipitation differences are within the same magnitudes as future projections for RCP8.5 (Fig. 3), future climate change may be represented by differences between P1 and P2 (for a shorter timescale). Results presented here suggest a shift from cold to temperate climate could change spring snowmelt from being the main recharge source. Instead, spring could be a period with less or no recharge. Due to warmer temperatures, the main recharge period could instead be in winter, as snow is increasingly replaced by rain, and reduced soil frost increases the infiltration capacity of the soil. The statistical test implies that annual groundwater recharge is reduced (increased end-of-year maximum and median depths, Table 2) as a result of this shift (Figs. 7 and 8). If these changes are representative of similar processes occurring over longer timescales, groundwater storage could generally be expected to decrease in Fennoscandia within the century. It is likely that similar effects may be seen in comparable hydrogeological and climatological settings, i.e. in areas with mainly local aquifers and cold (humid) climate zones. In addition to Fennoscandia, such settings can be found in large parts of northern Asia and east of the Rocky Mountains in North America (Richts et al., 2011; Fan et al., 2013; Beck et al., 2018).

#### 5.5. Approach limitations

The approach used here to associate hydraulic head class to hydrometeorology type has three main limitations. [1] The hydrometeorology classification is based on two simple models (estimating rain/snowmelt and PET) which may not always be representing the actual hydrometeorology state, and evapotranspiration is considered equal to PET. Factors affecting rain/snow and evapotranspiration magnitudes include, but are not limited to, land cover characteristics, wind and humidity (Healy and Cook, 2002; Taylor et al., 2012; Jasechko et al., 2014), and limitations caused by spatiotemporal resolution. [2] The approach is not designed to consider lag in groundwater-hydrometeorology responses, or responses at a less than biweekly temporal resolution. However, the plots showing hydraulic head fluctuations with the hydrometeorology classes (Fig. 5 and appendix D) indicate that even where lag occurs there exists at least partial overlap. Further, fast responses (< biweekly) are not expected to affect the results, since values are based on the median hydraulic head of 264 piezometers, over two 10-year periods. [3] The term 'effective precipitation' (Eq. (5)), does not describe actual groundwater recharge which would be measured in the field. Water may instead constitute runoff of different variations and surface or vadose zone storage. Vadose zone storage particularly may introduce an error for piezometers in Finland, as soil has an increasing water holding capacity north of 63° N, as compared to southern Finland (Hiederer, 2013a,b). The effect of runoff, surface storage and the connection of aquifer systems to rivers, varies spatially with hydrogeology and topography. Additionally, any recharge produced from effective precipitation may be insufficient to change the hydraulic head pattern (RH vs. DH), as it also depends on relative groundwater discharge.

The use of a group of piezometers to represent one grid cell of climate effects on groundwater may introduce further error. Piezometers in a group are not necessarily connected to the same aquifer as they are mostly small and disconnected in Fennoscandia. Piezometers therefore reflect local hydrogeological differences, independent of climate. Also, the seasonality of some piezometer hydrographs in a group are too dissimilar to include in the study, probably due to anthropogenic impacts. This suggests that in groups where only one piezometer is used (20 out of 74 groups, of which 17 are in Sweden, appendix A), such effects may be undiscovered.

## 6. Conclusions

The study analyses the effect of climate differences on the seasonality of groundwater fluctuations. The aim is to identify spatiotemporal differences in groundwater fluctuations and potential changes between two climatically different periods (1980–1989 and 2001–2010). Additionally, the aim is to quantify the effect on hydraulic heads. The approach consists of a qualitative assessment, associating hydraulic head fluctuations to hydrometeorology types, plus a quantitative assessment of differences in heads, expressed as depth to groundwater, between the selected periods. Thus, for the first time, annual groundwater recharge patterns are put in the context of shifting climate zones. The results indicate that:

- Intra-annual groundwater fluctuations in Fennoscandia are closely related to the 1986–2010 Köppen-Geiger climate zones as defined by Beck et al. (2018):
  - In temperate climate, intra-annual fluctuations in hydraulic heads are driven by rainy autumns and winters, and high evapotranspiration in spring and summer.
  - In cold climate, intra-annual fluctuations in hydraulic heads are driven by winter snowfall, snowmelt in spring, varying by rain and high evapotranspiration rates in summer, and rain in autumn.
- For the period 2001–2010, compared to 1980–1989, the duration of rain-associated rising hydraulic heads in winter is longer, as is the duration of declining hydraulic heads associated with high evapotranspiration in spring. Thus, the main recharge mechanism is shifting from spring snowmelt to winter rain.
- Depth to groundwater and the standard deviation has increased significantly for the period 2001–2010 compared to 1980–1989. This has implications for groundwater storage, indicating a decreasing trend over time. The link between rising vs. declining hydraulic heads and hydrometeorology types suggests this is a result of shorter snowmelt periods and longer high evapotranspiration rate duration. That is, higher temperatures have driven the change, irrespective of precipitation changes.
- Differences in groundwater seasonality and depth, between the periods 1980–1989 and 2001–2010, are pronounced along the climate transition zone (temperate to cold climate). This indicates that groundwater in Fennoscandia is highly influenced by, and vulnerable to short-term changes to, the climate regime.
- The time scales used here (10 years) are too short to draw solid conclusions on the impact of climate change on groundwater resources in Fennoscandia. However, the difference in hydrometeorology between 1980 and 1989 and 2001–2010 is in accordance with future projections for climate change in Sweden and Finland. Therefore, assuming these results may represent the impact on groundwater resources also over longer timescales, it is suggested that groundwater storage will mainly decrease in Fennoscandia.

Future work should focus on quantifying groundwater recharge and

storage by analysing hydraulic heads and stream discharge together. Note that a completely new selection of piezometers is necessary for such a study in Fennoscandia, as sites need to be chosen with careful consideration given to hydrogeological setting due to the generally poor hydraulic connection to streams. Additionally, a statistical analysis of driving climatology for the region could further clarify climate-groundwater interactions.

#### Declaration of Competing Interest

The authors declare that they have no known competing financial interests or personal relationships that could have appeared to influence the work reported in this paper.

#### Appendix A. Piezometer distribution per group

#### Acknowledgements

This study was funded by the Formas project number 2016-00513. We would like to thank Patrick Lachassagne, Sandra Lanini and two anonymous reviewers for the many comments that greatly improved this manuscript. We also thank two students, Amanda Lindgren and Amanda Jarefjäll, who did a preliminary study on the snowmelt model routine. Additionally, we thank Tinghai Ou and SMHI for assisting with the regional re-analysis model for Sweden. Research data for this article is available as follows: Swedish hydraulic heads are available at [www.sgu.se](http://www.sgu.se); Swedish meteorological data at [cds.climate.copernicus.eu](http://cds.climate.copernicus.eu); Finnish meteorological data at [avaa.tdata.fi](http://avaa.tdata.fi). For Finnish hydraulic head data contact Pekka Rossi.

**Table A1**

Distribution of piezometers per group (id) used in this study, including the median depth to groundwater. n corresponds to the number of piezometers in a group.

id	country	n	median depth below surface [m]
f_1352		5	0.81
f_385		9	1.17
f_2043		4	1.57
f_1854		1	4.03
f_1855		9	1.4
f_1274		7	0.96
f_3697		4	1.92
f_866		3	1.21
f_329		4	1.76
f_1526		5	1.31
f_2383		1	7.45
f_2113		4	0.54
f_2112		3	0.85
f_1312		5	3.3
f_1305		9	2.47
f_3453	Finland	3	4.38
f_491		4	6.25
f_131		5	1.4
f_1162		7	3.18
f_2401		11	6.23
f_783		1	4.77
f_784		2	5.20
f_830		2	5.71
f_2168		6	2.64
f_2167		6	4.25
f_3003		5	1.47
f_742		4	0.79
f_2360		10	1.81
f_3212		8	1.67
f_2465		5	1.47
f_471		8	1.05
s_1		1	3.76
s_2		1	4.27
s_3		1	7.69
s_21		1	1.37
s_22		1	0.32
s_29		3	1.23
s_32		6	7.79
s_40		5	7.47
s_45	Sweden	1	3.23
s_46		3	11.91
s_53		3	1.07
s_56		4	1.63
s_4		3	3.03
s_61		1	6.65
s_62		2	1.34
s_65		3	4.67

(continued on next page)

Table A1 (continued)

id	country	n	median depth below surface [m]
s_68		1	1.28
s_69		2	1.28
s_71		3	2.04
s_74		5	1.66
s_79		1	3.91
s_9		5	1.86
s_81		4	1.18
s_85		2	2.49
s_87		2	3.21
s_89		3	0.84
s_92		1	1.06
s_93		1	2.56
s_94		4	1.55
s_98		2	-0.45
s_115		3	0.63
s_117		5	1.09
s_123		2	1.79
s_126		1	15.14
s_131		6	2.68
s_137		2	7.73
s_139		1	1.52
s_150		2	0.8
s_152		3	3.71
s_155		1	0.91
s_156		1	1.04
s_157		1	2.76
s_158		1	1.48

## Appendix B. Snowmelt model

Using two parameters, air temperature  $T$  [°C] and precipitation  $P$  [mm], the model calculates five variables; snow accumulation (measured in snow water equivalents, SWE)  $A$  [mm], liquid water in the snowpack  $Sl$  [mm], snowmelt production in the snowpack  $M$  [mm], liquid water escaping the snowpack and liquid precipitation  $Q_{LW}$  [mm], and re/freezing of precipitation and liquid water in the snowpack  $R$  [mm].  $t$  indicates the time step in days.  $Q$  was also calculated to represent only snowmelt escape. This was done by following the same procedure, but precipitation was excluded in Eq. (B.6).

In the model, precipitation is classified as snow and refreezing, SWE accumulation and snowpack liquid are calculated if temperatures are lower than the temperature threshold as

$$\min(Sl_{t-1}, C_{FR} * C_M * (TT - T_t)) = R_t \quad (B.1)$$

$$A_{t-1} + P_t * S_{CF} + R_t = A_t \quad (B.2)$$

$$Sl_{t-1} - R_t = Sl_t \quad (B.3)$$

with  $C_{FR}$  being the refreezing coefficient [0.05],  $C_M$  is the degree-day factor [2.74 mm/°C/day],  $TT$  is the air temperature threshold [1 °C] and  $S_{CF}$  is the snowfall correction factor [0.7].

If the temperatures are higher than the temperature threshold, precipitation is classified as rain and any accumulated SWE is re-classified as melt according to

$$\min(A_{t-1}, C_M * (T_t - TT)) = M_t \quad (B.4)$$

$$A_{t-1} - M_t = A_t \quad (B.5)$$

$$Sl_{t-1} + P_t + M_t | Sl_{t-1} + M_t = Sl_t \quad (B.6)$$

If the liquid water in the snowpack exceeds the snow storage capacity multiplied by the snow accumulation ( $Sl_t > C_{WH} * A_t$ ), liquid water escaping the snowpack ( $Q_{LW}$ ) is calculated as

$$Sl_t - C_{WH} * A_t = Q_{LWt} \quad (B.7)$$

$$C_{WH} * A_t + M_t = Sl_t \quad (B.8)$$

with  $C_{WH}$  being the water holding capacity of a snowpack [0.1]. If there was no simulated snowpack,  $Sl_t$  and hence  $Q_{LW}$ , is equal to  $P_t$ .

## Appendix C. Raw data of piezometer groups

Median hydraulic head of each group plotted with individual piezometer and year hydraulic heads. Colours are to differentiate different piezometers and years. See Figs. C.1 and C.2.

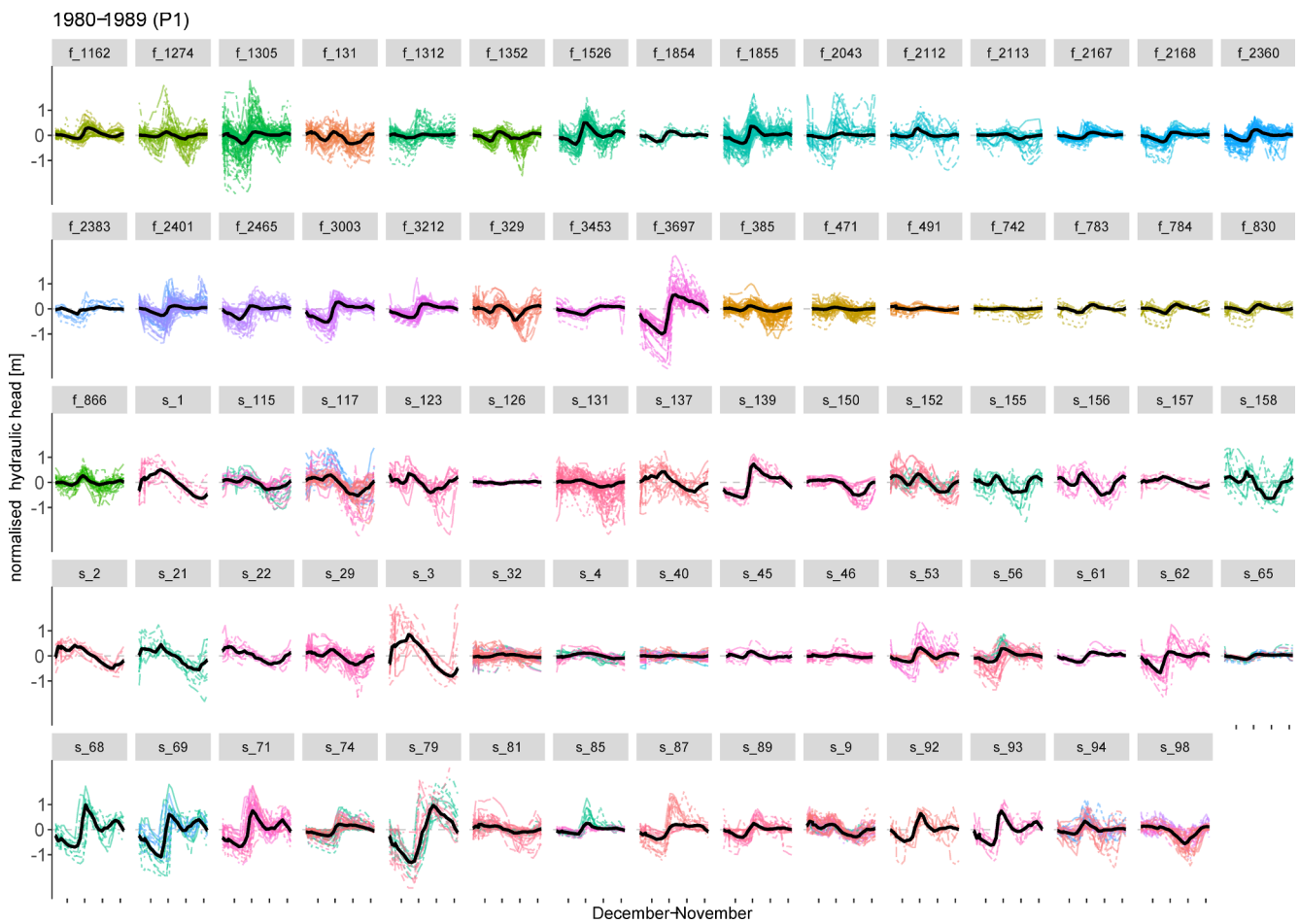


Fig. C1. The normalised hydraulic head in each group of piezometers for the period 1980–1989 (P1) in black, together with normalised heads for each piezometer and full year of data within that period which the median was calculated from. Colours indicate different piezometers, line pattern indicate different years.

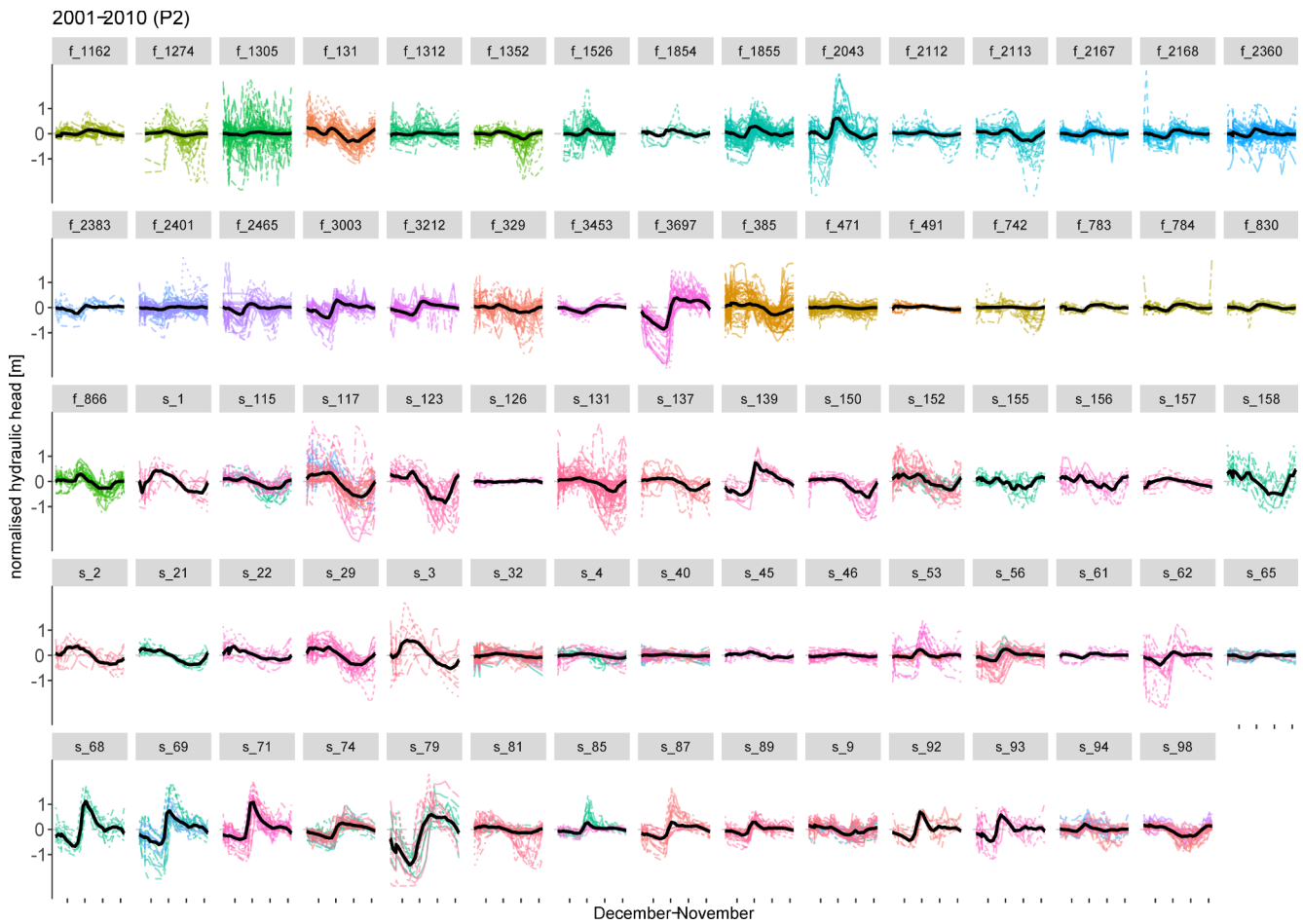


Fig. C2. The normalised hydraulic head in each group of piezometers for the period 2001–2010 (P2) in black, together with normalised heads for each piezometer and full year of data within that period which the median was calculated from. Colours indicate different piezometers, line pattern indicate different years.

Appendix D. Hydrometeorology types and hydraulic heads from P1 and P2

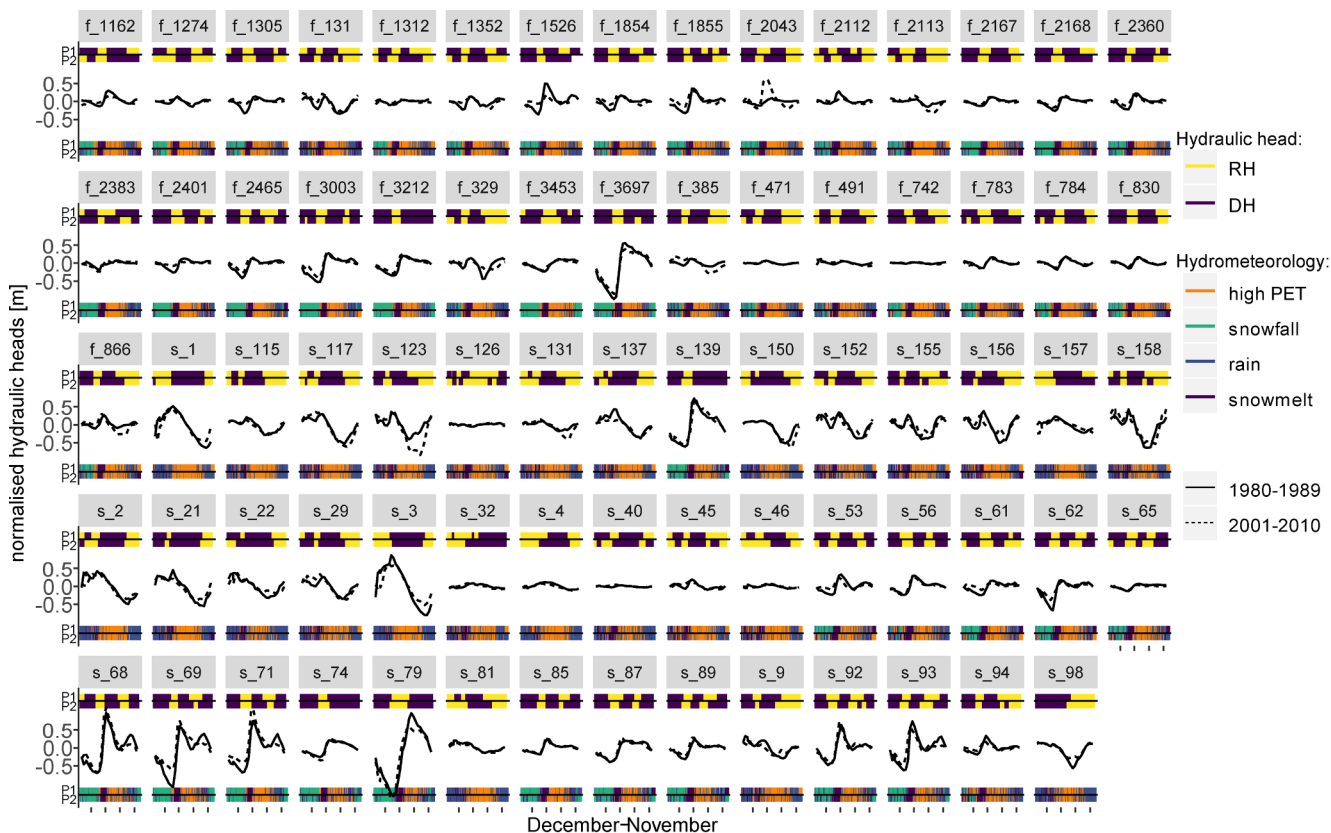


Fig. D1. Daily hydrometeorology and groundwater classifications plotted with the normalised hydraulic head fluctuations for all groups of piezometers. The hydraulic head classification is shown as columns per day at the top of the plots (RH vs. DH), and the hydrometeorology types at the bottom. P1 = 1980–1989, P2 = 2001–2010. RH = rising hydraulic heads, DH = declining hydraulic heads. Month ticks marks the beginning of each month.

Appendix E. All hydrometeorology-groundwater associations

The data analysis used to make Fig. E.1 is exactly the same as for Fig. 7. However, for Fig. 7, all counter-intuitive groundwater-hydrometeorology associations are removed. Fig. E.1 therefore presents all results from Fig. 7, and the additional links which, using our approach of a simple water budget equation (Eq. (5)), are not easily explained. These results cannot be explained in this study due to a combination of limitations, including the daily resolution of the groundwater-hydrometeorology associations, there being no data on soil frost, land cover and hydrogeological characteristics, and since no quantitative water budget calculations are made. There are possible explanations for why certain counter-intuitive links exist (which can be seen in Figs. 5 and D1). For example, groundwater could have the DH classification associated with rain, since effective rainfall (enough to produce recharge) is dependent on the infiltration capacity of the soil. Thus, for rainfall to be effective, not only do the conditions need to be energy- instead of water-limited (Eq. (5)), but it has been found that the magnitude of rainfall need to exceed a certain threshold for a certain number of days for recharge to be produced (e.g. Clilverd et al., 2011; Fu et al., 2019). However, since such conclusions cannot be made based on the approach used here, this figure (Fig. E.1) is not included in the main body of text.

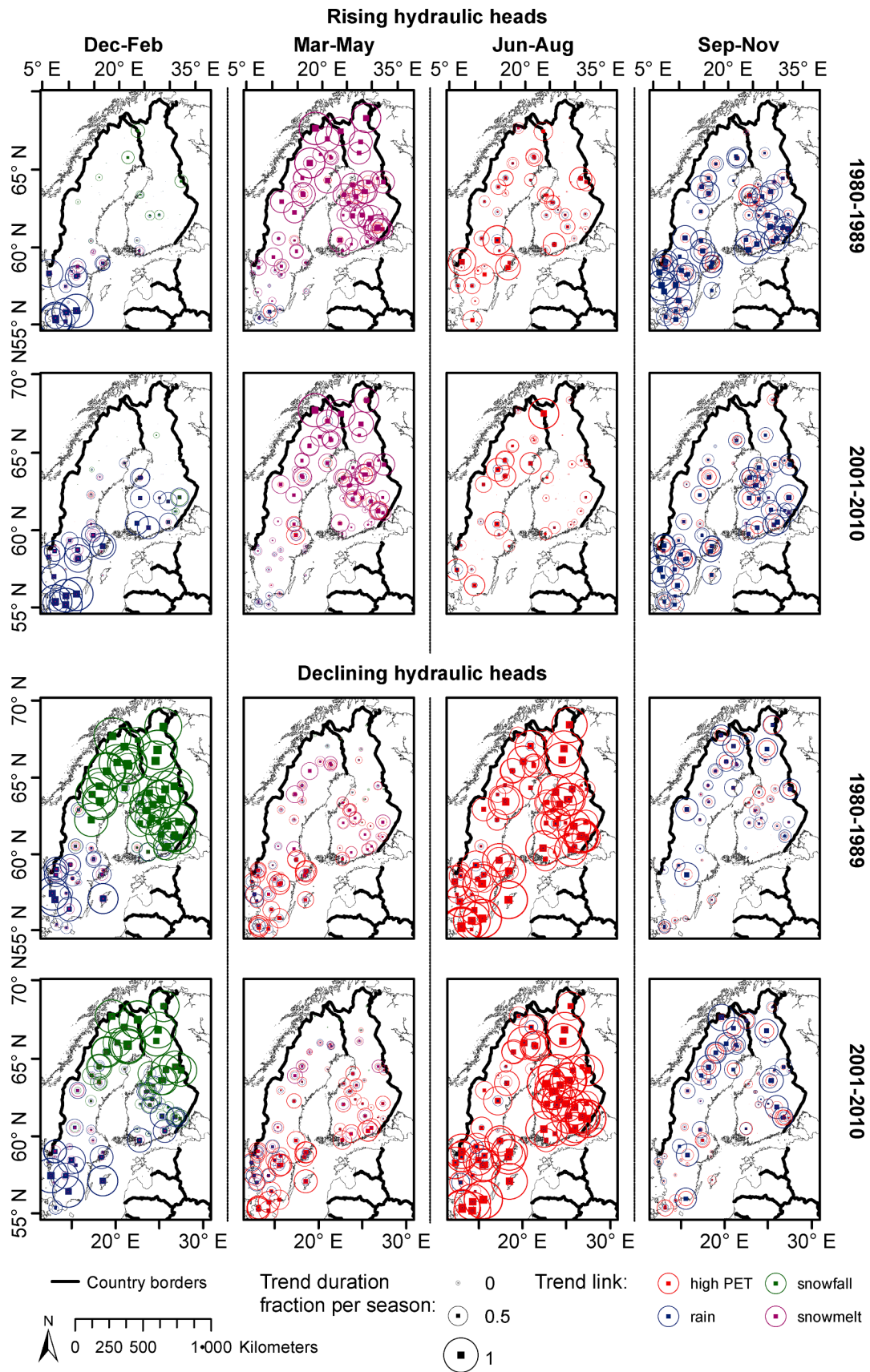


Fig. E1. All results realised from the groundwater-hydrometeorology associations. Each circle corresponds to one group of piezometers. Their size define the fraction per season (duration) with a specific groundwater-hydrometeorology association. The colour of the circle specifies the hydrometeorology type. Country borders are based on EuroGraphics and UN-FAO, @EuroGraphics.

## References

- Aalto, J., Pirinen, P., Jylhä, K., 2016. New gridded daily climatology of Finland: permutation-based uncertainty estimates and temporal trends in climate. *J. Geophys. Res.: Atmos.* 121 (8), 3807–3823. <https://doi.org/10.1002/2015jd024651>.
- Åberg, S., 2013. The highest shoreline of the Litorina Sea in Finland. University of Helsinki, Helsinki.
- Adrielsson, L., et al., 2006. *Geobiosfären en introduktion*. Studentlitteratur AB, Lund.
- Ala-aho, P., Rossi, P.M., Kløve, B., 2015. Estimation of temporal and spatial variations in groundwater recharge in unconfined sand aquifers using Scots pine inventories. *Hydrol. Earth Syst. Sci.* 19 (4), 1961–1976. <https://doi.org/10.5194/hess-19-1961-2015>.
- Allen, D.M., Stahl, K., Whitfield, P.H., Moore, R.D., 2014. Trends in groundwater levels in British Columbia. *Can. Water Resour. J.* 39 (1), 15–31.
- Asch, K., 2003. The 1:5 Million International Geological Map of Europe and Adjacent Areas: Development and Implementation of a GIS-enabled Concept. *Geologisches Jahrbuch, SA 3*, Stuttgart: E. Schweizerbart'sche Verlagsbuchhandlung.
- Baba, A., Tayfur, G., Gunduz, O., Howard, K., Fiedel, M., Chambel, A., 2011. In: *Climate Change and its Effects on Water Resources, Issues of National and Global Security*. Springer, Dordrecht. <https://doi.org/10.1007/978-94-007-1143-3>.
- Bauer, D.F., 1972. Constructing confidence sets using rank statistics. *J. Am. Stat. Assoc.* 67 (339).
- Beck, H.E., Zimmermann, N.E., McVicar, T.R., Vergopolan, N., Berg, A., Wood, E.F., 2018. Present and future Köppen-Geiger climate classification maps at 1-km resolution. *Sci. Data* 5, 180214. <https://doi.org/10.1038/sdata.2018.214>.
- Beguieria, S., Vicente-Serrano, S.M., 2017. SPEI: Calculation of the Standardised Precipitation-Evapotranspiration Index. R package version 1.7. < <https://CRAN.R-project.org/package=SPEI> >. (accessed on: May 20 2020).
- Bergström, S., 1976. Development and application of a conceptual runoff model for Scandinavian catchments, SMHI Report RHO 7, Norrköping.
- Bloomfield, J.P., Marchant, B.P., McKenzie, A.A., 2019. Changes in groundwater drought associated with anthropogenic warming. *Hydrol. Earth Syst. Sci.* 23 (3), 1393–1408. <https://doi.org/10.5194/hess-23-1393-2019>.
- Chen, D.L., Achberger, C., Raisanen, J., Hellstrom, C., 2006. Using statistical downscaling to quantify the GCM-related uncertainty in regional climate change scenarios: a case study of Swedish precipitation. *Adv. Atmos. Sci.* 23 (1), 54–60. <https://doi.org/10.1007/s00376-006-0006-5>.
- Chen, D., Chen, H.W., 2013. Using the Köppen classification to quantify climate variation and change: an example for 1901–2010. *Environ. Dev.* 6, 69–79. <https://doi.org/10.1016/j.envdev.2013.03.007>.
- Czilverd, H.M., White, D.M., Tidwell, A.C., Rawlins, M.A., 2011. The sensitivity of northern groundwater recharge to climate change: a case study in Northwest Alaska. *J. Am. Water Resour. Assoc.* 47 (6), 1228–1240. <https://doi.org/10.1111/j.1752-1688.2011.00569>.
- Condon, L.E., Atchley, A.L., Maxwell, R.M., 2020. Evapotranspiration depletes groundwater under warming over the contiguous United States. *Nat. Commun.* 11 (873). <https://doi.org/10.1038/s41467-020-14688-0>.
- Cuthbert, M.O., Gleeson, T., Moosdorf, N., Befus, K.M., Schneider, A., Hartmann, J., Lehner, B., 2019. Global patterns and dynamics of climate–groundwater interactions. *Nat. Clim. Change* 9 (2), 137–141. <https://doi.org/10.1038/s41558-018-0386-4>.
- Dierauer, J.R., Whitfield, P.H., Allen, D.M., 2018. Climate controls on runoff and low flows in mountain catchments of Western North America. *Water Resour. Res.* <https://doi.org/10.1029/2018wr023087>.
- Ebert, K., Hall, A.M., Klemm, J., Andersson, J., 2015. Unequal ice-sheet erosional impacts across low-relief shield terrain in northern Fennoscandia. *Geomorphology* 233, 64–74. <https://doi.org/10.1016/j.geomorph.2014.09.024>.
- Englund, J.O., Knutsson, G., Soveri, J., 1988. Studies on Groundwater Recharge in Finland, Norway and in Sweden. Proceedings of a Workshop, Mariehamn, Åland, Finland, 25–26 September 1986. Project within the Nordic Hydrological Programme 1984–1986, The Coordinating Committee for Hydrology in Norden, KOHYNO. Åland, Finland.
- Engström, J., Uvo, C.B., 2016. Effect of northern hemisphere teleconnections on the hydropower production in Southern Sweden. *J. Water Resour. Plann. Manage.* 142 (2), 05015008. [https://doi.org/10.1061/\(ASCE\)WR.1943-5452.0000595](https://doi.org/10.1061/(ASCE)WR.1943-5452.0000595).
- Fan, Y., Li, H., Miguez-Macho, G., 2013. Global patterns of groundwater table depth. *Science* 339 (6122), 940–943. <https://doi.org/10.1126/science.1229881>.
- Feiccabrin, J., Lundberg, A., 2008. *Precipitation phase discrimination in Sweden*. 65th Eastern Snow Conference, Fairlee, Vermont, USA.
- Fredén, C., 2009. *Berg och jord*. Sveriges Nationalatlas Förlag, ISBN: 978-91-87760-56-3.
- Fu, G., Crosbie, R.S., Barron, O., Charles, S.P., Dawes, W., Shi, X., Van Niel, T., Li, C., 2019. Attributing variations of temporal and spatial groundwater recharge: a statistical analysis of climatic and non-climatic factors. *J. Hydrol.* 568, 816–883. <https://doi.org/10.1016/j.jhydrol.2018.11.022>.
- Giese, M., Haaf, E., Heudorfer, B., Barthel, R., 2020. Comparative hydrogeology – reference analysis of groundwater dynamics from neighbouring observation wells. *Hydrol. Sci. J.* 65 (10). <https://doi.org/10.1080/02626667.2020.1762888>.
- Green, T.R., Taniguchi, M., Kooi, H., Gurdak, J.J., Allen, D.M., Hiscock, K.M., Treidel, H., Aureli, A., 2011. Beneath the surface of global change: impacts of climate change on groundwater. *J. Hydrol.* 405 (3–4), 532–560.
- Hamlet, A.F., Mote, P.W., Clark, M.P., Lettenmaier, D.P., 2007. Twentieth-century trends in runoff, evapotranspiration, and soil moisture in the Western United States. *J. Clim.* 20 (8), 1468–1486. <https://doi.org/10.1175/jcli4051.1>.
- Healy, R.W., Cook, P.G., 2002. Using groundwater levels to estimate recharge. *Hydrogeol. J.* 10 (1), 91–109. <https://doi.org/10.1007/s10040-001-0178-0>.
- Hiederer, R., 2013a. Mapping soil properties for Europe – spatial representation of soil database attributes. In: EUR26082EN Scientific and Technical Research series. Publications Office of the European Union, Luxembourg, pp. 47. <https://doi.org/10.2788/94128>.
- Hiederer, R., 2013b. Mapping soil typologies – spatial decision support applied to european soil database. In: EUR25932EN Scientific and Technical Research series. Publications Office of the European Union, Luxembourg, pp. 147pp. <https://doi.org/10.2788/8728>.
- Hinzman, L.D., et al., 2005. Evidence and implications of recent climate change in Northern Alaska and Other Arctic Regions. *Clim. Change* 72 (3), 251–298. <https://doi.org/10.1007/s10584-005-5352-2>.
- Irannezhad, M., Moradkhani, H., Kløve, B., 2019. Corrigendum to “spatio-temporal variability and trends in extreme temperature events in Finland over the recent decades: influence of northern hemisphere teleconnection patterns. *Adv. Meteorol.* 2019, 1–17. <https://doi.org/10.1155/2019/4857504>.
- Jang, S., Hamm, S.-Y., Yoon, H., Kim, G.-B., Park, J.-H., Kim, M., 2015. Predicting long-term change of groundwater level with regional climate model in South Korea. *Geosci. J.* 19 (3), 503–513. <https://doi.org/10.1007/s12303-015-0002-9>.
- Jasechko, S., et al., 2014. The pronounced seasonality of global groundwater recharge. *Water Resour. Res.* 50 (11), 8845–8867. <https://doi.org/10.1002/2014wr015809>.
- Jasechko, S., Wassenaar, L.L., Mayer, B., 2017. Isotopic evidence for widespread cold-season-biased groundwater recharge and young streamflow across central Canada. *Hydrol. Process.* 31 (12), 2196–2209. <https://doi.org/10.1002/hyp.11175>.
- Jenicek, S., Seibert, J., Zappa, M., Staudinger, M., Jonas, T., 2016. Importance of maximum snow accumulation for summer low flows in humid catchments. *Hydrol. Earth Syst. Sci.* 20 (2), 859–874. <https://doi.org/10.5194/hess-20-859-2016>.
- Jyrkama, M.I., Sykes, J.F., 2007. The impact of climate change on spatially varying groundwater recharge in the grand river watershed (Ontario). *J. Hydrol.* 338 (3–4), 237–250. <https://doi.org/10.1016/j.jhydrol.2007.02.036>.
- Jyväsjärvi, J., et al., 2015. Climate-induced warming imposes a threat to north European spring ecosystems. *Glob. Change Biol.* 21 (12), 4561–4569. <https://doi.org/10.1111/gcb.13067>.
- Kirkinen, J., Martikainen, A., Holttinen, I., Savolainen, I., Auvinen, O., Syri, S., 2005. Impacts on the energy sector and adaptation of the electricity network business under a changing climate in Finland, Finnish Environment Institute Mimeographs.
- Kjellström, E., Abrahamsson, R., Biberg, P., Jernbäcker, E., Karlbergs, M., Morel, J., Sjöström, Å., 2014. Uppdatering av det klimatvetenskapliga kunskapsläget. SMHI.
- Klemm, J., Stroeve, A.P., Lundqvist, J., 2008. Patterns of Quaternary ice sheet erosion and deposition in Fennoscandia and a theoretical framework for explanation. *Geomorphology* 97, 73–90. <https://doi.org/10.1016/j.geomorph.2007.02.049>.
- Kløve, B., et al., 2014. Climate change impacts on groundwater and dependent ecosystems. *J. Hydrol.* 518 (PB), 250–266. <https://doi.org/10.1016/j.jhydrol.2013.06.037>.
- Kløve, B., Kvitsand, H.M.L., Pitkänen, T., Gunnarsdóttir, M.J., Gaut, S., Gardarsson, S.M., Rossi, P., Miettinen, I., 2017. Overview of groundwater sources and water-supply systems, and associated microbial pollution, in Finland, Norway and Iceland. *Hydrogeol. J.* 25, 1033–1044.
- Kottek, M., Grieser, J., Beck, C., Rudolf, B., Rubel, F., 2006. World Map of the Köppen-Geiger climate classification updated. *Meteorol. Z.* 15 (3), 259–263. <https://doi.org/10.1127/0941-2948/2006/0130>.
- Kovalevskii, V.S., 2007. Effect of climate changes on groundwater. *Water Resour.* 34 (2), 140–152. <https://doi.org/10.1134/s0097807807020042>.
- Kurylyk, B.L., MacQuarrie, K.T.B., 2013. The uncertainty associated with estimating future groundwater recharge: a summary of recent research and an example from a small unconfined aquifer in a northern humid-continental climate. *J. Hydrol.* 492, 244–253. <https://doi.org/10.1016/j.jhydrol.2013.03.043>.
- Lee, B., Hamm, S.-Y., Jang, S., Cheong, J.-Y., Kim, G.-B., 2013. Relationship between groundwater and climate change in South Korea. *Geosci. J.* 18 (2), 209–218. <https://doi.org/10.1007/s12303-013-0062-7>.
- Lidmar-Bergström, K., Bonow, J.M., Japsen, P., 2013. Stratigraphic Landscape Analysis and geomorphological paradigms: Scandinavia as an example of Phanerozoic uplift and subsidence. *Global Planet. Change* 100, 153–171. <https://doi.org/10.1016/j.gloplacha.2012.10.015>.
- Luoma, S., Okkonen, J., 2014. Impacts of future climate change and Baltic Sea level rise on groundwater recharge, groundwater levels, and surface leakage in the Hanko aquifer in Southern Finland. *Water-Sui.* 6 (12), 3671–3700. <https://doi.org/10.3390/w6123671>.
- Meixner, T., et al., 2016. Implications of projected climate change for groundwater recharge in the western United States. *J. Hydrol.* 534, 124–138. <https://doi.org/10.1016/j.jhydrol.2015.12.027>.
- Okkonen, J., Kløve, B., 2011. A sequential modelling approach to assess groundwater–surface water resources in a snow dominated region of Finland. *J. Hydrol.* 411 (1–2), 91–107. <https://doi.org/10.1016/j.jhydrol.2011.09.038>.
- Peel, M.C., Finlayson, B.L., McMahon, T.A., 2007. Updated world map of the Köppen-Geiger climate classification. *Hydrol. Earth Syst. Sci.* 11.
- Richts, A., Struckmeier, W.F., Zaepke, M., 2011. WHYMAP and the groundwater resources map of the World 1:25,000,000. In: Jones, J.A.A. (Ed.), *Sustaining Groundwater Resources: A Critical Element in the Global Water Crisis*. Springer, Netherlands, Dordrecht, pp. 159–173. [https://doi.org/10.1007/978-90-481-3426-7\\_10](https://doi.org/10.1007/978-90-481-3426-7_10).
- Rinderer, M., Meerveld, H.J., McGlynn, B.L., 2019. From points to patterns: using groundwater time series clustering to investigate subsurface hydrological connectivity and runoff source area dynamics. *Water Resour. Res.* 55 (7), 5784–5806. <https://doi.org/10.1029/2018wr023886>.
- Rubel, F., Kottek, N., 2010. Observed and projected climate shifts 1901–2100 depicted by world maps of the Köppen-Geiger climate classification. *Meteorol. Z.* 19 (2),

- 135–141. <https://doi.org/10.1127/0941-2948/2010/0430>.
- Rubel, F., Brugger, K., Haslinger, K., Auer, I., 2017. The climate of the European Alps: shift of very high resolution Köppen-Geiger climate zones 1800–2100. *Meteorol. Z.* 26 (2), 115–125. <https://doi.org/10.1127/metz/2016/0816>.
- Ruosteenoja, K., Julhae, K., Kaemaeraainen, M., 2016. Climate projections for Finland under the RCP forcing scenarios. *Geophysica* 51 (1), 17–50.
- Scheliga, B., Tetzlaff, D., Nuetzmann, G., Soulsby, C., 2018. Groundwater dynamics at the hillslope–riparian interface in a year with extreme winter rainfall. *J. Hydrol.* 564, 509–528. <https://doi.org/10.1016/j.jhydrol.2018.06.082>.
- Scibek, J., Allen, D.M., 2006. Modeled impacts of predicted climate change on recharge and groundwater levels. *Water Resour. Res.* 42 (11). <https://doi.org/10.1029/2005wr004742>.
- Scibek, J., Allen, D.M., Cannon, A.J., Whitfield, P.H., 2007. Groundwater–surface water interaction under scenarios of climate change using a high-resolution transient groundwater model. *J. Hydrol.* 333 (2–4), 165–181. <https://doi.org/10.1016/j.jhydrol.2006.08.005>.
- Seibert, J., 2005. HBV light User's Manual. Department of Physical Geography and Quaternary Geology, Stockholm University.
- Seibert, J., Vis, M.J.P., 2012. Teaching hydrological modeling with a user-friendly catchment-runoff-model software package. *Hydrol. Earth Syst. Sci.* 16 (9), 3315–3325. <https://doi.org/10.5194/hess-16-3315-2012>.
- SGU, 2015. Produkt Högsta Kustlinjen. SGU, Göteborg.
- SMHI, [no date]. Klimatscenerier. Accessible via: < <https://www.smhi.se/klimat/framtidens-klimat/klimatscenerier/sweden/nation/rcp85/year/precipitation> > . (accessed on: March 13 2020).
- Staudinger, M., Seibert, J., 2014. Predictability of low flow – an assessment with simulation experiments. *J. Hydrol.* 519, 1383–1393. <https://doi.org/10.1016/j.jhydrol.2014.08.061>.
- Stoll, S., Hendricks Franssen, H.J., Barthel, R., Kinzelbach, W., 2011. What can we learn from long-term groundwater data to improve climate change impact studies? *Hydrol. Earth Syst. Sci.* 15 (12), 3861–3875. <https://doi.org/10.5194/hess-15-3861-2011>.
- Stroeven, A.P., et al., 2016. Deglaciation of Fennoscandia. *Quat. Sci. Rev.* 147, 91–121. <https://doi.org/10.1016/j.quascirev.2015.09.016>.
- Sultana, Z., Coulibaly, P., 2011. Distributed modelling of future changes in hydrological processes of Spencer Creek watershed. *Hydrol. Process.* 25 (8), 1254–1270. <https://doi.org/10.1002/hyp.7891>.
- Surfleet, C.G., Tullos, D., Chang, H., Jung, I.W., 2012. Selection of hydrologic modeling approaches for climate change assessment: a comparison of model scale and structures. *J. Hydrol.* 464–465, 233–248. <https://doi.org/10.1016/j.jhydrol.2012.07.012>.
- Surfleet, C.G., Tullos, D., 2013. Uncertainty in hydrologic modelling for estimating hydrologic response due to climate change (Santiam River, Oregon). *Hydrol. Process.* 27 (25), 3560–3576. <https://doi.org/10.1002/Hyp.9485>.
- Taylor, R.G., et al., 2012. Ground water and climate change. *Nat. Clim. Change* 3 (4), 322–329. <https://doi.org/10.1038/Nclimate1744>.
- Thornthwaite, C.W., 1948. An approach toward a rational classification of climate. *Geogr. Rev.* 38 (1), 55–94.
- Undén, P., 2017. Uncertainties in Ensembles of Regional Reanalyses, Sveriges Meteorologiska och Hydrologiska Institut, Norrköping.
- Van Loon, A.F., 2015. Hydrological drought explained. *Wiley Interdiscip. Rev.: Water* 2 (4), 359–392. <https://doi.org/10.1002/wat2.1085>.
- Wang, H., Tetzlaff, D., Buttle, J., Carey, S., Laudson, H., McNamara, J., Spence, C., Soulsby, C., 2018. Climate-phenology-hydrology interactions in northern high latitudes: assessing the value of remote sensing data in catchment ecohydrological studies. *Sci. Total Environ.* 656. <https://doi.org/10.1016/j.scitotenv.2018.11.361>.
- Ymparisto, 2019. Groundwater in Finland. Finnish Environment Institute. Accessible via: < [https://www.ymparisto.fi/en-US/Waters/Protection\\_of\\_waters/Groundwater\\_protection/Groundwater\\_in\\_Finland](https://www.ymparisto.fi/en-US/Waters/Protection_of_waters/Groundwater_protection/Groundwater_in_Finland) > . (accessed on: October 16 2019).